



# HHS Public Access

Author manuscript

*Adv Mater Technol.* Author manuscript; available in PMC 2021 March 01.

Published in final edited form as:

*Adv Mater Technol.* 2020 March ; 5(3): . doi:10.1002/admt.201900720.

## Biosensors for Personal Mobile Health: A System Architecture Perspective

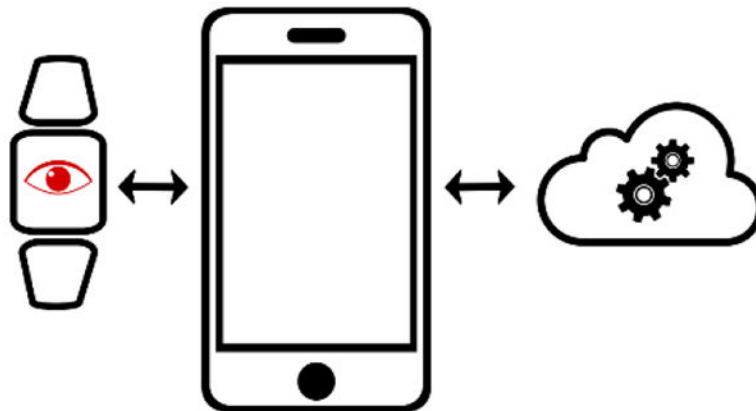
Siddarth Arumugam, David A.M. Colburn, Samuel K. Sia

Department of Biomedical Engineering, Columbia University, 10027 New York, United States

### Abstract

Advances in mobile biosensors, integrating developments in materials science and instrumentation, are fueling an expansion in health data being collected and analyzed in decentralized settings. For example, semiconductor-based sensors are enabling measurement of vital signs, and microfluidic-based sensors are enabling measurement of biochemical markers. As biosensors for mobile health are becoming increasingly paired with smart devices, it will become critical for researchers to design biosensors – with appropriate functionalities and specifications – to work seamlessly with accompanying connected hardware and software. This article describes recent research in biosensors, as well as current mobile health devices in use, as classified into four distinct system architectures that take into account the biosensing and data processing functions required in personal mobile health devices. We also discuss the path forward for integrating biosensors into smartphone-based mobile health devices.

### Graphical Abstract



The review examines recent advances in biosensors for collecting personal health measurements. We pay particular attention to how biosensors can be designed to be integrated with smartphones. Examples of biosensors for each of the four system architectures (for biosensing and data processing) are discussed.

## Keywords

biosensors; diagnostics; mHealth; smartphones; data processing

---

## 1. Introduction

Innovations in materials and instrumentation are enabling miniaturization of biosensors for health measurements to be collected and analyzed in decentralized settings, outside of a clinical laboratory.<sup>[1–3]</sup> For example, advances in semiconductor-based microelectromechanical systems have led to the proliferation of high-quality, low-power mobile sensors across a range of modalities<sup>[4]</sup>, including health measurements such as vital signs. For biochemical measurements, different organic and inorganic materials for microfluidics have facilitated development of devices with finely tuned physical, chemical, and optical properties,<sup>[5]</sup> enabling recapitulation of complex chemical assays at the point of care (POC).<sup>[5, 6]</sup> Furthermore, nanomaterials such as carbon nanotubes and graphene have driven development of new types of biosensors,<sup>[7]</sup> including applications in detecting cancer biomarkers<sup>[8]</sup> or monitoring glucose levels.<sup>[9]</sup>

As biosensors are increasingly aimed for use directly by consumers and patients, they are being offered in the familiar form factor of smartphones. In 2018, over 1.56 billion smartphones were sold worldwide,<sup>[10]</sup> with about 35% of the global population owning a smartphone<sup>[11]</sup> and 81% of the U.S. owning smartphones.<sup>[12]</sup> As such, smartphones could serve as attractive mobile health (mHealth) devices due to their form factor and inbuilt features and, due to their ubiquity, could help democratize healthcare and bridge the gap between patients and healthcare professionals.<sup>[13]</sup> The Internet of Medical Things (IoMT) framework, also known as healthcare Internet of Things (IoT), constitutes a connected infrastructure of medical devices that can collect, analyze, and transfer data using networking technologies.<sup>[14]</sup> Smartphone-based diagnostic and mHealth systems, by virtue of their inbuilt sensors and connectivity features, are an integral part of this developing IoMT framework.<sup>[15]</sup> To serve as mHealth devices, smartphones must be augmented with two additional features: biosensing, as discussed above, and health data processing, as made possible by the increasing performance of mobile processors.<sup>[16]</sup> For data processing, connectivity and cloud computing also offer the possibility to offload computationally intensive processing to powerful servers.<sup>[17]</sup>

With an increasing number of demonstrations of mHealth devices featuring the smartphone as an integral component,<sup>[3]</sup> new possibilities are arising of smart connected health<sup>[18]</sup> and a new digital health ecosystem. As a consequence, the possible constructions of biosensors are increasing at a bewildering pace. For example, the biosensor could be constructed as a separate microfluidic chip that can communicate, as a wireless accessory, with the smartphone. However, it is also possible to build biosensing – along with computing and connectivity – into the smartphone itself, thereby minimizing additional hardware, improving portability, and potentially reducing cost.<sup>[19]</sup>

Previous reviews have examined the utility of smartphones for clinical diagnostics.<sup>[1, 13, 20, 21]</sup> Due to the abundance of diagnostic applications that rely on an optical readout,

many of these reviews focus on the inbuilt complementary metal-oxide-semiconductor (CMOS) camera sensor. The smartphone has also been used to develop low-cost, portable microscopes capable of achieving up to 800X magnification.<sup>[22]</sup> Further, with software augmentation, resolutions rivaling those of table-top microscopes are possible.<sup>[23]</sup> Since connectivity is a key feature of smartphones that facilitates interfacing with external sensors and devices, Kwon *et al.* and Xu *et al.* reviewed application that used either inbuilt sensors or external sensors connected to the smartphone through wired or wireless means.<sup>[24, 25]</sup> In addition, for detection of analytes, Sun and Hall reviewed off-phone electrochemical biosensors for POC applications.<sup>[19]</sup> However, since multiple biosensing modalities are typically coordinated together for the end user via a single smart device, there will be a need to examine different types of biosensing functions through a single lens. Also, it will be necessary to examine biosensing in combination with data processing, as it is the combination of these functions – which will feedback into the design of the biosensors – that will generate actionable insight, especially with advances in artificial intelligence (AI) and the expanding volume of health data.<sup>[26]</sup>

In this review, we examine recent smartphone-based mHealth devices, with an emphasis on developments since 2014. Similar to early perspectives on mHealth that had outlined system architectures involving the biosensing and data processing capabilities,<sup>[27]</sup> we propose a “full-stack” perspective that examines the recent advances in biosensors alongside accompanying data processing capabilities. As the landscape of biosensors for mHealth devices is rapidly expanding, we will focus on some of the key literature that covers a range of sensing modalities alongside data processing methods that have been adapted to the smartphone, at both the academic and commercial level. Other reviews have covered biosensing modalities and applications in detail.<sup>[1, 13, 19, 20, 24, 25, 28, 29]</sup>

## 2. Four System Architectures of Biosensors for Personal mHealth

Although the technical specifications and form factors of smartphone-based mHealth devices will change over time, they will exhibit two defining and immutable features: a technology for sensing health parameters and software for processing this sensor data to extract actionable information. Hence, we classify the range of smartphone-integrated health devices based on the criteria of data acquisition and data processing (Figure 1a). Specifically, we categorize the devices based on whether the biosensing function is built on- or off-phone, and if the data processing is performed locally on the phone or via the cloud in a server. Here we refer to “local processing” to be data processing that occurs either on the smartphone (as commonly understood) or on a standalone biosensing accessory. For “server processing”, we refer to data processing that takes place on the cloud (as commonly understood) or on a nearby computer that communicates with the smartphone or a standalone biosensing accessory. Cloud services commonly used for this purpose currently include Google Cloud Platform, Microsoft Azure, and Amazon Web Services. Examples of devices, including commercial mHealth devices in use as well as major categories of smartphone-integrated biosensors being developed in academic research, are shown for each system architecture (Figure 1b).

Smartphones can use either on-phone sensors or communicate with external, off-phone sensors. The location of the biosensing function (either on the phone or off the phone) is an important design criterion for researchers in mHealth devices, as the biosensing capabilities may be limited by the smartphone-supplied component. Modern smartphones contain numerous internal sensors for data acquisition, including, but not limited to, cameras, ambient light sensors, microphones, accelerometers, gyroscopes, magnetometers, and barometers. While the types of sensors built into smartphones continue to expand,<sup>[30]</sup> only a subset of these have demonstrated utility in healthcare applications. In addition to increased portability, a major advantage of using internal sensors for data acquisition is the availability of mature software tools for interfacing with the hardware, removing the need for *ab initio* firmware development. Further, as the sensors have already been optimized for the phone, there is no need to design the pre-processing electronic circuits.<sup>[25]</sup> However, as smartphones are not currently equipped with all the relevant health sensor modalities, an integrated smartphone biosensor is currently restricted in the types of health data they can gather. Nevertheless, smartphones possess connectivity technology, such as USB, Bluetooth, WiFi, and near-field communication (NFC), that enable them to interface with a large number of external biosensors to expand their range of signal acquisition capabilities. This flexibility introduces a challenge of interfacing with a multitude of external sensors which may necessitate designing a large number of customized hardware and software to collect and transmit the data to the smartphone, increasing cost and development time.

Biosensors that measure vital signs and other biophysical signals are made primarily from silicon using standard semiconductor device fabrication techniques. The camera and ambient light sensors are designed using CMOS technology that makes use of both N- and P-type metal-oxide-semiconductor field-effect transistors (MOSFETs).<sup>[31]</sup> In these devices, silicon acts as the semiconductor with polysilicon and silicon oxide acting as the conductor (“metal”) and the insulator (“oxide”), respectively. Another major class of sensor are based on microelectromechanical systems (MEMS). In these devices, the integrated electronics are fabricated with the same CMOS technology as the camera sensors.<sup>[32]</sup> The mechanical structures of these devices are typically made from silicon and polysilicon. Silicon is used because of the mature fabrication process pioneered by the microelectronics industry while polysilicon is used due to its ideal mechanical properties at the microscale.<sup>[33]</sup> Typical on- and off-phone specifications and fabrication materials for common biosensors are summarized in Table 1.

For measuring levels of biochemical and chemical analytes, many point-of-care biosensors employ microfluidics to carry out sample handling and small-volume reactions. In many instances, the readout is a colorimetric or fluorometric signal which is measured using an external photodiode or the smartphone camera’s CMOS sensor. The materials used most frequently for these applications are those that exhibit optical transparency or are of a format where color changes are easily visible, can be easily machined facilitating quick fabrication, are biocompatible, and are inexpensive. These materials fall under the three broad categories: polymers, inorganic materials, and paper-based.<sup>[34, 35]</sup> Common polymer materials include polydimethylsiloxane (PDMS), poly (methyl methacrylate) (PMMA), cyclic olefin copolymer (COC), and polycarbonate (PC). Examples of inorganic materials

include glass and ceramic. The list of materials and specific advantages of each material are listed in Table 1.

After acquiring the raw sensor signal, it is necessary to transform the data to yield actionable health information using either local or server processing. When designing the data processing pipeline, a primary consideration is minimizing the “time to answer”, here defined as the time between signal acquisition and the output of processed health information to the user. Current smartphones contain a System-on-Chip (SoC) with integrated multi-core processor and graphics processing unit (GPU), memory, onboard storage, as well as multiple connectivity interfaces.<sup>[36]</sup> The general-purpose processor typically has between 2 and 8 cores, allowing for effective multi-tasking, with clock speeds reaching up to nearly 3 GHz while the GPUs are approaching nearly 1 TFLOPS with single-precision floating-point numbers.<sup>[37]</sup> Thus, in many circumstances, smartphones can run the full data processing pipeline locally with tolerable latency. However, the computing power of smartphones still fall below that offered by dedicated workstations or cloud servers. Thus, smartphones may not be suited for data processing that requires significant computing power because the processing latency may grow to intolerable levels. To overcome this limitation, smartphones can leverage their built-in connectivity features to transfer sensor data to a more powerful server and offload the more computationally expensive parts of the data pipeline. After the processing is completed, the server can transmit the results back to the smartphone, where it can be displayed to the user. While the data transmission introduces another source of latency, server processing is often faster than performing the computation locally.<sup>[17]</sup> Thus, applications with either large amounts of data or complex analytics often use server-assisted data processing.

Next, we review recent advances and devices that fall under each of the four system architectures.

### **2.1. Integrated: on-phone biosensing with local data processing**

The first system architecture features an internal biosensor built into a smartphone, along with the SoC for fully integrated sensing and data processing. These devices often have the smallest form factor of the four system architectures. While smartphones are equipped with a wide variety of inbuilt sensors, only a subset of these sensors, such as imaging sensors and microphone, are commonly used in diagnostic applications. Applications that use internal sensors can be further subdivided based on whether or not an adapter is required to ensure the proper functionality of the system. Adapters are mainly required for applications where the alignment of the sensor and the sample is crucial, such as in cases of smartphone-based microscopy. The applications listed here have been subgrouped based on whether an additional adapter is needed for the functionality of the system or not. With the advancements in the quality of camera sensors, lenses, and image analysis software, the performance gap between smartphone cameras and conventional high-end cameras is shrinking.<sup>[1, 20]</sup> This increase in camera performance has facilitated the use of the smartphone-acquired images for diagnostic purposes.

**Adapter-dependent applications:** Kalwa *et al.* demonstrated a fully-integrated smartphone application for the detection of melanoma at the POC.<sup>[38]</sup> The user takes an image of the target skin site using the smartphone with a 10× detachable lens, which is then subjected to a number of image processing steps such as preprocessing, segmentation, and feature extraction. A support vector machine classifier is then used to determine whether the image is indicative of a malignant or benign lesion. Using the PH2 dermoscopic image database, the authors demonstrated an area under the receiver operating characteristic curve (AUC) of 0.85 with 80% sensitivity and 90% specificity. MoleScope™, a commercially available smartphone attachment for dermoscopy allows the user to obtain magnified images of the skin with controlled lighting.<sup>[39]</sup> The images can be stored and viewed on a computer using a web platform and can be shared with a dermatologist, thereby facilitating teledermatology. While there are concerns regarding the accuracy of smartphone sourced images when compared to a dermatoscope,<sup>[40]</sup> improved image processing algorithms and better smartphone attachments may increase the reliability of the platform. Xu *et al.* developed a smartphone-based platform for the acquisition and analysis of retinal fundus images directly on the phone.<sup>[41]</sup> The smartphone is attached to an adapter which helps position the system in front of the eye being examined. The authors detected no significant difference in the performance when lower-quality smartphone images were used when compared to those obtained with fundus cameras. They evaluated their proposed system on the DRIVE and STARE databases and found AUC, sensitivity, and specificity values of 0.959, 0.786, and 0.955, respectively, on the DRIVE database and 0.959, 0.825, and 0.931, respectively, on the STARE database.

Smartphones, with their small form factor, imaging capability, and connectivity, have made portable microscopy possible. Lee and Yang developed a compact, chip-scale smartphone microscope using ambient illumination.<sup>[42]</sup> Their microscopy method is based on shadow imaging, where a sample is directly placed on the image sensor. When coupled with on-phone, super-resolution reconstruction from multiple images taken at different illumination angles, sub-micron resolution over an ultra-wide field-of-view is possible. The authors have demonstrated the utility of the microscope by imaging microscopic samples, blood cells in smears, microspheres, and freshwater algae in pond water. Orth *et al.* developed a dual-mode smartphone microscope capable of operating using a camera flash or ambient light for brightfield and darkfield imaging.<sup>[43]</sup> They devised a clip-on 3D printed attachment that easily attaches to the smartphone (Figure 2a) and demonstrated the utility of the system in imaging cell nuclei in unlabelled cells, cattle sperm, and zooplankton. An interesting application of the mobile phone microscope was devised by Fletcher and group where they quantified the amount of microfilaria in whole blood samples to determine those patients who can receive ivermectin treatment.<sup>[44]</sup> The smartphone video microscope can function with whole blood, with no additional sample preparation or staining steps, and produces the answer in 2 minutes. The authors validated the performance of the microscope using blood samples from 33 patients and showed that the results were comparable to conventional thick smear counts (94% specificity; 100% sensitivity). Kanakasabapathy *et al.* developed a smartphone-based semen analyzer for POC male infertility screening.<sup>[45]</sup> The system consists of a disposable microfluidic device for handling the semen samples and an optical attachment for the smartphone to facilitate image magnification and device alignment



(Figure 2b). The smartphone application was designed to capture images, automatically analyze, and report the results in less than 5 seconds with comparable performance to the more expensive and labor-intensive computer-assisted semen analysis system. The coefficient of variation when testing preclinical samples was found to be 4.5%. A total of 350 unprocessed clinical semen samples were analyzed and the system provided the semen quality evaluation, based on the World Health Organization (WHO) guidelines, with ~98% accuracy.

Researchers have also demonstrated smartphone-based spectrometers for quantification of the readout from colorimetric assays. Halvorsen *et al*, developed a rapid smartphone-based neonatal diagnostic test for measuring the levels of lactate dehydrogenase (LDH) from whole blood samples.<sup>[46]</sup> The POC system consists of a disposable paper strip with dried-down chemical reagents which produce the colorimetric readout. The strip is mounted on an injection-moulded plastic cartridge and is placed within a box holder to ensure optimal spacing between the smartphone camera and the cartridge. Plasma from whole blood is separated using filter papers, and the smartphone captures an image of the cartridge. The RGB values are extracted from the image and the calculated concentration of LDH is displayed on the screen within three minutes. The mean LDH ( $\pm$ SD) were found to be comparable between the POC system ( $551 \pm 280$  U/L) and standard laboratory analysis ( $552 \pm 249$  U/L).

Priye *et al*. developed a platform for smartphone-based diagnosis of mosquito-borne viral infections using the methods of reverse transcription-loop-mediated isothermal amplification (RT-LAMP) and quenching of unincorporated amplification signal reporters (QUASR).<sup>[47]</sup> They built a portable LAMP detection platform that interfaced with a smartphone to facilitate in-field diagnostics. The LAMP box consisted of (i) a heating module powered by a 5V source (ii) assay reaction housing module (iii) optical-detection/image analysis module. A smartphone application, Lamp2Go, connected to the LAMP box via Bluetooth and allowed the smartphone to control the heater and LEDs. The smartphone camera is used to capture an image of the reaction tubes which are analyzed on the phone via an app. The authors developed a colorimetric detection algorithm to decouple brightness information from color by mapping the pixel values from the RGB space to the CIE color space. Their platform is a field-deployable test system capable of multiplexed viral RNA detection, which could be used to diagnose viral infections from different sample matrices without the need for extensive sample preparation steps. They demonstrated the viability of their system by detecting Zika virus RNA down to 100 particle forming units per mL that was spiked in blood, urine, and saliva human sample matrices.

Liu and group developed a “smart-connected cup” for carrying out rapid, connected molecular diagnostics.<sup>[15]</sup> Their smartphone-based platform combines bioluminescent assay in real-time and LAMP, wherein the luciferin produces bioluminescent light (Figure 2c) which is detected by the smartphone camera. A major advantage of this method is that it removes the need for an excitation source and optical filters. The authors developed an Android application to 1) monitor luciferin emission in real-time, 2) quantify emission intensity, and 3) determine the concentration of the target. The final results are displayed on the screen and, if required, can be transmitted to a remote secure server. Additionally, the

application records the GPS location of each test to facilitate spatiotemporal disease mapping via a custom-designed website. They demonstrated the performance of the platform by detecting the Zika virus in urine and saliva samples with a sensitivity of 5 particle forming units per urine sample and HIV in blood samples within 45 minutes.

Using the microphone built into the smartphone, researchers have also built acoustics-based diagnostic biosensors. Thap *et al.* developed a lung function test using variable frequency complex demodulation method-based lung function parameter estimation using an audio signal recorded from the smartphone's built-in microphone with an add-on mouthpiece attachment<sup>[48]</sup> (Figure 2d). A smartphone application for the iPhone 5S was developed using Objective-C for the estimation of the forced expiratory volume in 1 s/ forced vital capacity (FEV1/FVC) ratio. Once the audio signal had been recorded, the application took 5 seconds to visualize the FEV1/FVC ratio estimation. The authors demonstrated that their system could estimate the FEV1/FVC ratio with an absolute error and root mean squared error of  $4.5\% \pm 3.4\%$  and  $5.5\%$ , respectively, for healthy subjects and  $10.3\% \pm 10.6\%$  and  $14.5\%$ , respectively, for patients with chronic obstructive lung disease. However, the authors also noted that, even with the mouthpiece attachment, there were variations in the angle at which users exhaled into the microphone, causing errors in the estimation of FEV<sub>1</sub>, FVC, and peak expiratory flow.

**Adapter-free applications:** Force sensors that are built into recent smartphone models have enabled diagnostic and biosensing applications. Chandresekhar *et al.* developed a smartphone application that uses the inbuilt photoplethysmogram (PPG) and force sensors along with the front-facing camera to estimate the subject's blood pressure.<sup>[49]</sup> The subject presses their finger against the sensor and the application's inbuilt algorithm displays the PPG value and the measured blood pressure in real time on the screen. The bias and precision errors were  $-4.0$  and  $11.4$  mm Hg for systolic blood pressure and  $-9.4$  and  $9.7$ -mm Hg for diastolic blood pressure. Compared to a finger-cuff device, the error was 2 mm Hg higher. On the other hand, the application yielded more "try-again" messages and the blood pressure measurements were not as repeatable as their previous system<sup>[50]</sup>, which used dedicated off-phone sensors, due to variability in the positioning of the fingertip.

In addition, stand-alone smartphone applications using user-entered data have been developed for diagnosis and monitoring of disease progression. The examples listed here are those in the areas of eye care and mental health. Oculocare's Alleye.io and Vital Art and Science's myVisionTrack are both FDA approved smartphone applications that have been developed to ascertain the severity and progression of age-related macular degeneration.<sup>[51]</sup> Alleye.io works by asking users to align three dots with one of their eyes closed and generates a score based on their performance. myVisionTrack has similar functionality, where the user selects the least circular object from a number of circular shapes. Based on their ability to delineate shapes, the application produces a score. Rutter *et al.* developed DelApp, a smartphone application for the assessment of attention deficit disorder in older hospitalized patients.<sup>[52]</sup> The application serves to be an objective assessment tool that is easily administered at the bedside setting. It comprises an arousal assessment (scored between 0 and 4) followed by a sustained attention task (scored between 0 and 6). The final



score is a total out of 10, where 10 indicates normal attention. The test is usually completed within 5 min.

In addition to diagnostics and health monitoring, applications have been developed to aid daily activities and wellness. One such example is the SmartHear application, developed by Yu-Cheng Lin and group<sup>[53]</sup>, for assisting individuals with mild to moderate hearing loss. The hearing assistive application was a smartphone-based implementation of the personal frequency modulation system. It mainly consisted of a smartphone running a mobile application paired to a Bluetooth headset. The speaker spoke into the smartphone's microphone, and audio was transmitted to the Bluetooth headset worn by the listener. In a 5-person user survey conducted by the authors, they found that the SmartHear system was favorably received due to its low cost, accessibility, and the low stigma associated with its usage.

## 2.2. Cloud: on-phone biosensing with data processing on a server

This system architecture deals with devices with built-in biosensors for health data acquisition and data processing that is done on a cloud server or on an external computer. Server processing is used either due to the complexity of the analysis, which makes it infeasible to run on the smartphone, or in those instances where the application is geared towards use in locations where the network connectivity is inadequate. In many instances, server processing is performed initially to establish the proof of concept, after which the algorithm is optimized for local deployment. We have grouped the applications here based on whether or not an external adapter is required for the functioning of the device.

**Adapter-dependent applications:** Yetisen *et al.* demonstrated the use of injectable dermal tattoo sensors that undergo a colorimetric change upon exposure to variations in pH, glucose, and albumin concentrations.<sup>[54]</sup> Images of the dermal sensors were taken with a smartphone and analyzed in MATLAB to quantify the color change (Figure 3a). The tattoo sensors yielded a standard error in aqueous solutions and in ex-vivo tissues of 0.3 pH and 0.2 pH, respectively, for pH sensing, 0.3 mmol/L and 0.2 mmol/L, respectively, for glucose measurement, and 0.2 g/L and 0.1 g/L, respectively, for albumin measurement. In a similar vein, Ozcan and group developed a smartphone-based microplate reader for carrying out enzyme-linked immunosorbent assays at the POC.<sup>[55]</sup> The system consists of a 3D printed attachment which holds a 96 well plate and an LED array for the illumination of the plate. Optical fibers carried the light to the smartphone camera mounted on the same attachment (Figure 3b). The image was then transmitted to online servers for analysis, and the results are sent back to the phone in approximately one minute. The authors validated the performance of their system using tests for mumps, measles, HSV-1, HSV-2 and achieved an accuracy of 99.6%, 98.6%, 99.4%, and 99.4%, respectively. Ding *et al.* developed a smartphone-based multispectral imager with an optical resolution of 100  $\mu\text{m}$  and demonstrated its performance by non-invasively carrying out nevus lesion diagnosis and dental plaque detection.<sup>[56]</sup> The housing for the multispectral imaging chip and the optical components was 3D printed and attached to the smartphone.

Uthoff *et al.* developed a dual-modality, POC oral cancer screening device.<sup>[57]</sup> The system contains interchangeable probes to facilitate both intraoral and whole cavity imaging through autofluorescence imaging and white light imaging. The illumination is provided by six 405 nm Luxeon UV U1 LEDs, for the autofluorescence imaging, and four 4000 k Luxeon ZES LEDs, for the white light imaging. The LEDs are controlled by a custom Android application via a Bluetooth connected microcontroller unit. The captured data is sent to a cloud server for analysis and automated classification using convolutional neural networks. Using 170 white light and autofluorescence image pairs, they were able to train and validate their convolution neural network, which was shown to have an AUC of 0.91, sensitivity of 0.85, specificity of 0.89, positive predictive value of 0.88, and negative predictive value of 0.85. Ozcan and group have demonstrated that smartphone microscopy can benefit from deep learning.<sup>[23]</sup> Images taken by a conventional smartphone camera can be modified using deep learning algorithms to improve their spatial resolution, signal-to-noise ratio, and color response. It has been demonstrated that with this software augmentation, the image quality is comparable to images taken by a bench-top microscope with a 20X objective lens (Figure 3c).

**Adapter-free applications:** An example of an adapter-free application is the SMARTtest app, which our lab has developed, to accompany the INSTI duplex HIV and syphilis self-testing kit.<sup>[58]</sup> The application provides the user with a list of instructions to carry out the test, prompts the user and guides them into taking a picture of the kit, transfers the image to a cloud server where the image is analyzed, and receives the results from the server which can then be saved or shared by the user. This application is geared towards removing user subjectivity in the interpretation of results, and allow users to share the results with their partner or healthcare provider. Wang *et al.* developed a paper-based colorimetric sensing platform for the detection of glucose and uric acid.<sup>[59]</sup> The color change could either be detected by the naked eye or, for a more quantitative analysis, by using a smartphone to take images of the kit, which were then analyzed offline using the ImageJ software. The sensor had a linear response from 0.01 mM to 1.0 mM for uric acid detection and from 0.02 mM to 4.0 mM for glucose detection. The limit of detections were 0.003 mM and 0.014 mM for uric acid and glucose, respectively.

The company Healthy.io has developed an FDA approved smartphone-based home urinalysis kit.<sup>[60]</sup> The user purchases the kit, which contains the dipstick, urine container, and a color board for calibration purposes. The user, after performing the test, takes a picture of the dipstick inserted into the color board. The image is sent to a cloud server for analysis, and the results are sent to the user within a couple seconds. The results are also shared with the health care practitioner. Luo *et al.* have demonstrated the ability to estimate blood pressure from facial videos recorded using a smartphone camera using transdermal optical imaging (TOI).<sup>[61]</sup> The recorded videos were then analyzed using machine learning algorithms to estimate the blood pressure from the captured data. The authors showed that their models were able to predict systolic blood pressure with an accuracy of 94.8%, diastolic blood pressure with an accuracy of 95.7%, and pulse pressure with an accuracy of 95.7%. The bias  $\pm$  standard deviation values were  $0.39 \pm 7.3$  mm Hg,  $-0.26 \pm 6.0$  mm Hg, and  $0.52 \pm 6.42$  mm Hg for systolic pressure, diastolic pressure, and pulse pressure,

respectively. While the study measured only people with normal blood pressure under rest conditions and with uniform controlled lighting, the paper demonstrated the utility of using TOI to estimate blood pressure with reasonable accuracy. FibrCheck, developed by Qompium, is an FDA approved and CE certified application for the detection of atrial fibrillation.<sup>[62]</sup> It functions by acquiring a PPG measurement from the user's finger using the camera and the camera's flash. The recording takes a minute to complete, after which the data is sent to a server for further analysis. Sharma *et al.* demonstrated the smartphone-based imaging of fluorescent magnetic nanoparticles, where the images were analyzed on the cloud.<sup>[63]</sup> The group demonstrated the efficacy of the system by measuring the level of the prostate-specific antigen and achieved a limit of detection of 100 pg/mL, which was measured in less than 60 seconds.

Narayan *et al.* demonstrated that it is possible to detect disturbed and normal breathing patterns from ambient sounds recorded by an unmodified smartphone microphone.<sup>[64]</sup> The authors studied 91 patients undergoing polysomnography by using a Samsung Galaxy S5 smartphone placed less than 1 meter from the head of the bed to record ambient sounds. The recorded sound files were exported for analysis in MATLAB. Using the validation cohort, the authors showed that their algorithm performed with a c-statistic of 0.87 when compared to whole-night polysomnography. The study demonstrated that using unmodified smartphone recordings, without specialized equipment or physical contact with the patient, it is possible to identify the acoustic signatures of sleep-disordered breathing. Steth IO is an FDA approved smartphone-based digital stethoscope that is composed of 3 elements: 1) a smartphone case with a built-in waveguide, 2) a smartphone application, and 3) a cloud platform for identification of abnormal heart and lung sounds.<sup>[65]</sup> The waveguide is used to filter out unwanted sounds and feed the amplified heart and lung sounds directly into the smartphone's microphone. By keeping the smartphone against the patient's chest, the application can visualize the phonocardiogram in real time. ResApp is a smartphone application designed for the diagnosis of respiratory disease using only the smartphone microphone.<sup>[66]</sup> The application records cough sounds as the user coughs into the microphone and sends them to a cloud server for analysis.

hearScreen is a smartphone application developed by hearX for the purpose of detecting hearing loss.<sup>[67]</sup> The user is asked to plug in headphones to the audio jack and listen to numbers that are called out in the presence of artificial noise. The user enters the numbers they hear using the touchscreen input, and the process is repeated 23 times. The data is then uploaded to the cloud for processing, after which the hearing score is sent back to the phone within a few seconds. The entire test takes a minute or two to complete. Studies conducted in primary health clinics have shown that the application performs with acceptable sensitivity and specificity in a time-efficient manner.<sup>[68]</sup> Faurholt-Jepsen *et al.* demonstrated using smartphone data to identify patients with bipolar disorder.<sup>[69]</sup> The specially designed MONARCA software automatically collected smartphone data, such as the number of outgoing and incoming calls and text messages per day, duration of phone calls (min/day), the number of times the smartphones' screen was turned on or off per day, and the duration the smartphone screen was on per day. Using this data from a cohort of 29 patients with bipolar disorder and 37 healthy individuals, the authors were able to identify patients with bipolar disorder with a positive predictive value of 0.88 and a negative predictive value of

0.52. This application shows the potential use of smartphone data as a diagnostic behavioral marker.

### 2.3. Tethered: off-phone biosensing with local data processing

This system architecture features devices with the biosensing function off the smartphone, but with data processing taking place on the smartphone. The main advantage of this system architecture is the flexibility of working with a large range of sensors, thus enabling the monitoring of numerous health targets that would otherwise be infeasible with a smartphone alone. Further, as the data processing takes place locally, these devices typically retain functionality when not connected to the internet. As a result, this class of device is potentially more attractive for use in low-resource settings with intermittent access to the internet. A common paradigm for this system architecture is for the sensing and processing to occur on the external device with the results transmitted to the smartphone. Thus, in some cases, the smartphone can be viewed as a peripheral instrument that augments the functionality of an external device rather than being an integral component. However, even for these smartphone-optional devices, integration with the smartphone is often necessary to enable more advanced functionality.

The most common academic examples of this classification have been developed for biochemical assays, particularly those that use an electrochemical readout.<sup>[70]</sup> Electrochemical analysis is widely used for quantitative analyte detection. Electrochemical analysis can typically be classified as either potentiometric, amperometric, or impedimetric where measures of voltage, current, and impedance are related to analyte concentrations, respectively.<sup>[71]</sup> A recent example of potentiometric sensing is the smartphone-interfaced chip for biological sex identification demonstrated by Deng *et al.*<sup>[72]</sup> The device consisted of an external electrochemical chip that connected to a smartphone using microUSB, and was controlled by an application on the phone. The device used cyclic voltammetry to detect creatine kinase (CK) and alanine transaminase (ALT) via quantitative detection of NADH consumption. In an assay for CK detection, the system had a limit of detection (LOD) of 100 U/L and dynamic range of 100 to 3200 U/L. In the pure ALT assay, the system had a LOD of 10 U/L and a dynamic range of 10 to 640 U/L. By utilizing a joint CK-ALT assay, the system was shown to discriminate between male and female serum samples, with AUC, sensitivity, and specificity of 0.874, 88.3%, and 88.9%, respectively.

An example of amperometric readout is the system developed by Guo for the monitoring of blood  $\beta$ -ketones for early detection of diabetic ketoacidosis.<sup>[73]</sup> The device consists of a smartphone-powered electrochemical analyzer that uses disposable test strips to detect blood ketone concentration from fingerstick whole blood (Figure 4a). After addition of a drop of whole blood, the  $\beta$ -hydroxybutyrate dehydrogenase integrated with the test strip drives the conversion of  $\beta$ -hydroxybutyrate to acetylacetic acid. This cascade subsequently drives the oxidation of NADH into NAD<sup>+</sup>, which can be detected amperometrically using the electrochemical analyzer. After mapping the current to the concentration of  $\beta$ -hydroxybutyrate, the results are transmitted to the smartphone via USB. The system was demonstrated to have a LOD of 0.001 mmol/L and a dynamic range of 0.001 mmol/L to

6.100 mmol/L. Further, the device was shown to have excellent agreement with benchtop electrochemical analyzer.

An impedimetric-based example is the smartphone-based system for the detection of volatile organic compounds (VOCs) developed by Liu *et al.*<sup>[74]</sup> The system used interdigital electrodes that interfaced with a mobile impedance sensing device with results transmitted to the smartphone via Bluetooth in real time. The electrodes had been modified with graphene and ZnO such that increasing VOC concentration resulted in an increase in the conductivity of the electrodes due to the reduction of adsorbed oxygen and subsequent transfer of free electrons to the electrode. This change in conductivity was measured by the impedance sensing device and used to measure the concentration of VOCs. The system was shown to have a LOD of 1.56 ppm for acetone with a linear response range up to 10 ppm. Further, the system was able to discriminate acetone from other VOCs, like formaldehyde, via impedance spectroscopy. Impedance readout was also adapted for blood cell counting in a work by Talukder *et al.*<sup>[75]</sup> They developed a portable cytometer capable of detecting the small change in impedance from cells flowing past the electrode. The minimum change in impedance that the sensor could detect using 3  $\mu\text{m}$  beads was 0.032%. The sensing was performed by custom lock-in amplifier circuit interfaced with an Arduino Uno microcontroller. The sampled data was transmitted to the smartphone via Bluetooth for processing.

As the components required for each of these modalities are similar, a recent study by Escobedo *et al.* developed a general-purpose device that could perform both amperometric and potentiometric readouts.<sup>[76]</sup> The device consisted of a general-purpose electrochemical analyzer that was powered and controlled by a smartphone via NFC. Amperometric operation was demonstrated for the quantification of glucose, where the system had a LOD 0.024 M and dynamic range of 0.065 to 0.750 M. Similarly, potentiometric operation was demonstrated by measuring pH, where the system was shown to have a dynamic range of 3 to 9. This device was also designed for electrochemiluminescence applications. This technique combines the principles of electrochemistry with chemiluminescence where the application of a voltage drives the electrochemistry reaction that subsequently triggers chemiluminescence.<sup>[77]</sup> This functionality was demonstrated with the quantification of hydrogen peroxide, where the system had a LOD of 0.03 mM and dynamic range of 0.62 to 100 mM. However, this modality alone uses the smartphone's internal camera sensor for readout of the chemiluminescence. Kassal *et al.* developed a smart bandage which could measure the levels of uric acid<sup>[78]</sup> and the pH<sup>[79]</sup> to monitor the status of wound healing. Uric acid sensing was achieved by screen printing an amperometric sensor directly onto a wound dressing which facilitated the chronoamperometric sensing of uric acid. The data was wirelessly transferred via radio-frequency identification (RFID) or NFC to computer, tablet, or a smartphone. The performance of the uric acid sensor was compared with that of the CHI 440 electrochemical sensor and there was high agreement between the two instruments ( $R^2 = 0.9967$ ) with a sensitivity coefficient of  $-2.4 \text{ nA}/\mu\text{M}$ .<sup>[78]</sup> For the sensing of pH, the authors were able to construct a bandage with immobilized cellulose particles covalently attached to a pH sensing dye. An optoelectronic probe quantified the pH value and stored it on the device. The data could then be transmitted via RFID to a smartphone or computer. The performance of the pH sensor was compared with that of a reference pH meter and the

difference in the measured pH values was used to determine the accuracy and precision of the smart bandage. The accuracy and precision values were found to be 0.08 pH units and 0.05 pH units, respectively, demonstrating the ability of the pH sensor to accurately measure the pH values in the ranges tested.<sup>[79]</sup>

Smartphone-based biochemical assays have also been developed that use external optics. One example is the mChip platform described by Laksanasopin *et al.* for POC diagnosis of infectious disease (Figure 4b).<sup>[80]</sup> This platform consists of a smartphone dongle, powered and controlled via the 3.5 mm audio jack, that replicated all components of a benchtop enzyme-linked immunosorbent assay (ELISA) and was validated with whole blood. Using venipuncture whole blood the dongle achieved a sensitivity and specificity of 100% and 91%, respectively for HIV, 77% and 89%, respectively for treponemal syphilis, and 80% and 82%, respectively for nontreponemal syphilis. Li *et al.* developed a smartphone-assisted microfluidic chemistry analyzer for the detection of three markers indicative of diabetes and hyperlipidemia status: glucose, triglyceride, and total cholesterol.<sup>[81]</sup> The serum samples were added to a microfluidic chip and the color changes were measured using a custom analyzer with a built-in optical system which was under the control of a smartphone. The data generated by the analyzer is wirelessly transmitted via Bluetooth to a smartphone for result determination using previously established standard curves. The authors compared the performance of their system with that of an automatic chemistry analyzer and achieved high coefficients of determination between the two sets of results for all the analytes measured: 0.969, 0.966, and 0.969 for glucose, triglyceride, and total cholesterol, respectively. In addition to biochemical assays, off-phone optical readout has been described by Das *et al.* using a mini-spectrometer for skin cancer diagnosis.<sup>[82]</sup> The device was composed of a MEMS spectrometer controlled by an Arduino microcontroller that incorporated an additional Bluetooth module, for transmission of the data to the smartphone for analysis, and discriminated between normal skin and cancerous lesions via the reflectance spectra. The device demonstrated a resolution of 10  $\mu\text{m}$ . The smartphone blood pressure monitor described by Chandrasekhar *et al.*<sup>[50]</sup> is another example of off-phone optical readout. This device uses a PPG sensor coupled with a thin-filmed, capacitive force sensor to measure blood pressure using a modified oscillometric technique (Fig 4c). Compared to an oscillometric arm cuff device, the system was shown to have a mean absolute error of  $3.3 \pm 8.8$  mmHg for systolic pressure and  $5.6 \pm 7.7$  mmHg for diastolic pressure.

Off-phone sensing with client-side processing has also been explored for acoustic-based applications. For example, Reyes *et al.* describe a system that used an off-phone electret microphone as an acoustic sensor for detection of crackle sounds in pneumonia patients.<sup>[83]</sup> The sensor interfaced with the smartphone via the 3.5 mm audio jack where the acquired acoustic signal was processed using a time-varying autoregressive algorithm to automatically detect crackles (Figure 4d). When validated with synthetic data injected with both fine and coarse crackles, the system was found to have an average accuracy, sensitivity and specificity of approximately 81%, 89%, and 99%, respectively. However, when tested with real patients, these metrics decreased. In another work, Jayatilake *et al.* developed a device for automatic analysis of swallowing sounds for dysphagia diagnosis.<sup>[84]</sup> The device uses a neck-worn microphone to record the swallowing sound which is then processed using an on-phone algorithm for detection of both dry and wet swallows. Dry swallow detection



was validated using 8 subjects with 71 dry swallow episodes where the system was found to have a precision of 83.7% and recall of 93.9%. Similarly, wet swallow detection was validated using 31 subjects with 92 wet swallow episodes where the accuracy was 79.3%. Smartphones have also been employed in mobile ultrasound. Huang *et al.* described a smartphone-based system for blood flow measurement using Doppler ultrasound.<sup>[85]</sup> The device used a 10-MHz ultrasonic sensor, for monitoring blood flow, interfaced with an analog processing circuit. The pre-processed Doppler signal was then transmitted to the smartphone using the 3.5 mm audio jack for visualization and spectrogram analysis. Initial calibration was performed using a Couette flow phantom with porcine blood under pulsatile conditions. The system was validated *in vivo* by comparing the arterial blood flow measure of a rat with those acquired using a commercial ultrasound duplex scanner. The mobile ultrasound system was found to have good agreement with a commercial duplex scanner.

Stopczynski *et al.* developed the Smartphone Brain Scanner (SBS2) application which combines an off-the-shelf EEG cap with a smartphone resulting in a fully-portable real-time 3D EEG imaging system.<sup>[86]</sup> The EEG recordings collected by the cap were wirelessly transmitted to an Android phone for processing and imaging reconstruction. A validation study was carried out by McKenzie *et al.* to assess the performance of the application. The reconstructed EEG waveform was used for detecting epileptiform abnormalities and was compared to a standard EEG.<sup>[87]</sup> It was found that SBS2 yielded sensitivity and specificity values of 39.3% and 94.8% respectively with a positive prediction value of 0.71 and a negative predictive value of 0.82. The main limitation in the performance of the system was its low to moderate sensitivity when compared to standard EEG.

In addition to these technologies in development, there are a number of commercial devices within this system architecture. The most prominent examples are the fitness trackers and smartwatches offered by Fitbit,<sup>[88]</sup> Apple,<sup>[89]</sup> and Samsung,<sup>[90]</sup> among other commercial vendors. While these products may contain a host of different sensors, common configurations contain an accelerometer and a photoplethysmogram sensor. After acquiring the raw sensor signal, proprietary algorithms are used to estimate activity and heart rate. Further, some devices apply additional processing to track other metrics, including distance travelled, calories burned, or sleep state. The processed data is then shared with the smartphone where it can be visualized and stored for later analysis. However, despite their popularity, there are concerns over the accuracy and clinical relevance of these devices.<sup>[91]</sup>

A recent development in this space is the integration of electrodes to enable on-demand recording of clinical-grade electrocardiogram (ECG). While preceded by AliveCor's KardiaBand, a prominent example today is the Apple Watch, where ECG capability was introduced with the Series 4 model; however, other ECG-capable smartwatches are in development. Further, mobile ECG devices are not limited to the watch form-factor. For example, the AliveCor KardiaMobile<sup>[92]</sup> consists of a pad with two electrodes that can be clipped to the smartphone. Despite the differences in form-factor, all of these devices operate by acquiring a short ECG recording, typically around 30-seconds in length, and then transmitting it to the smartphone for analysis. Some products, like the KardiaMobile and KardiaBand, have developed algorithms to analyze the ECG recording to detect arrhythmias. AliveCor's atrial fibrillation detection algorithm was shown to have a sensitivity and

specificity of 96.6% and 94%, respectively, when used with the KardiaMobile.<sup>[93]</sup> When used with the KardiaBand, the algorithm demonstrated a sensitivity and specificity of 93% and 84%, respectively.<sup>[94]</sup> Another ECG example is the QardioCore.<sup>[95]</sup> Whereas the previous products discussed collect a short ECG recording, the QardioCore continuously records ECG via wearable chest electrodes that wirelessly transmit to the smartphone. In addition to ECG, the QardioCore continuously monitors heart rate, body temperature, and physical activity. To date, no study has examined the clinical utility of the QardioCore.

“Elemark lipid check” is a smartphone-based in vitro diagnostic device for the measurement of three lipid biomarkers: total cholesterol (TC), high density lipoprotein (HDL), and triglyceride (TG).<sup>[96]</sup> The device consists of an analyzer, test strips, and a compatible smartphone. The analyzer physically attaches to the smartphone and the operation of the analyzer is controlled via an app. Yun *et al.* compared the performance of elemark lipid check with that of the hospital-grade AU5800 Analyzer from Beckman Coulter.<sup>[97]</sup> The comparison study showed that the elemark lipid check demonstrated high correlation with that of reference test  $R = 0.97$  for TC,  $R = 0.97$  for HDL, and  $R = 0.99$  for TG. Additionally, 99.1% of the measured TC concentration values at 100 mg/dL or higher were within  $\pm 15\%$  of the reference results, 100% of measured HDL concentration values less 100 mg/dL were within  $\pm 10$  mg/dL of the reference results, and 96.7% of the measured TG concentration values at 100 mg/dL or higher were within  $\pm 15\%$  of the reference results.

Another set of examples of this system architecture are the smart scales offered by Withings,<sup>[98]</sup> FitBit,<sup>[88]</sup> and others. While the most basic models typically only track the user’s weight and body mass index over time, the more advanced models provide estimates of body composition and pulse wave velocity. To measure body composition, the scales use bioelectrical impedance analysis. Integrated electrodes are used to pass a small current through the user and the impedance is recorded. As the measure of electrical impedance is known to relate to total body water and fat-free body mass, the scales can calculate body composition using the measured weight in conjunction with the user’s height and sex.<sup>[99]</sup> To measure pulse wave velocity, the scales use both ballistocardiography and impedance plethysmography.<sup>[100]</sup> By analyzing the ballistocardiogram, the scale can detect the opening of the aortic valve. Similarly, analysis of the plethysmogram signal yields the arrival time of the blood pressure pulse wave at the foot. By dividing by the distance between the foot and the heart, estimated by the user’s height, the scale can estimate the velocity of the pulse wave. Like fitness trackers, these products primarily use the smartphone as a peripheral that offers another means to visualize the data as both the sensing and processing are performed on the scale.

Numerous other smartphone-integrated smart devices have been developed that satisfy the criteria for this classification. Examples range from smart thermometers and blood pressure monitors, like the QardioArm<sup>[101]</sup> or Omron HeartGuide,<sup>[102]</sup> to wireless electroencephalograms (EEG) for guided meditation,<sup>[103]</sup> and wearable respiratory monitors for early detection of asthma attacks.<sup>[104]</sup> In addition to these biophysical measures, smartphone-integration has been implemented in devices used for tracking biochemical targets, most notably blood glucose concentration via the smart glucose meters marketed by iHealth Labs<sup>[105]</sup> and DarioHealth,<sup>[106]</sup> among others. After measuring the user’s blood

glucose levels using standard electrochemical techniques, these devices transmit the reading to the smartphone, enabling efficient and accurate self-monitoring. In addition to discrete monitors, smartphone-based features have been incorporated into all of the latest models of continuous glucose monitors. Complimentary to these products, Companion Medical developed the InPen, the first FDA approved smart insulin pen.<sup>[107]</sup> Whereas the smart glucose meters automatically log blood glucose concentration, the InPen monitors the amount of insulin delivered. By automatically logging insulin dosage to the smartphone for later review, smart insulin pens are expected to improve clinical outcomes by facilitating treatment optimization.<sup>[108]</sup> Smartphones are also being used for portable ultrasound, such as the Philips Lumify<sup>[109]</sup> and the Butterfly iQ.<sup>[110]</sup> Both devices offer clinical-grade imaging capabilities at dramatically reduced cost and have been cleared by the FDA for multiple clinical applications, including fetal and obstetric exams. Critically, these products are marketed primarily to healthcare professionals and hospitals, indicating that the healthcare industry will adopt smartphone-integrated health devices if the value is clear.

#### 2.4. Hub: off-phone biosensing with data processing on a server

The last system architecture we consider features devices where biosensing takes place off the smartphone, and where data processing takes place on an external computer or a remote server. Here, the smartphone serves primarily as a data collection hub and user interface. Examples of devices that fit these criteria are more limited than the other system architectures, possibly because current mHealth devices with off-phone biosensors typically perform measurements that do not require computationally expensive data processing. However, as the latest AI techniques continue to be successfully applied to problems in healthcare,<sup>[111]</sup> more devices may make use of the sophisticated data processing available via the cloud to analyze the collected data to provide personalized predictive analytics.

Philips *et al.* developed the WristO<sub>2</sub>, a wrist-worn device for the estimation of SpO<sub>2</sub>.<sup>[112]</sup> They used the MAX30102 reflective pulse oximeter and the MPU9250 IMU sensor for collecting data together with an Adafruit FLORA microcontroller for data alignment. A smartphone running an Android application was connected to the microcontroller via a USB connection. This USB connection served to power each device as well to read and visualize the signals from all the connected sensors. The application then saved the readings and sent them to a remote database for offline data processing. The authors demonstrated the reliability of SpO<sub>2</sub> sensing by showing a reduction in the RMSE value to 1.5% brought about by the integration of the features extracted from the IMU sensor with that of the reflective pulse oximeter.

Despite the relative infancy of AI in healthcare, a number of commercial products within this system architecture have already made this transition. One example is the Bluetooth equipped blood glucose meter from One Drop.<sup>[113]</sup> While the core functionality of the device, blood glucose measurement, occurs locally, one of its more interesting features, the “Automated Decision Support”, is made possible with cloud processing using advanced AI algorithms. After taking a blood glucose measurement, the reading is transmitted to One Drop cloud network where it is analyzed and compared to over one billion other glucose measurements. Once processed, the Automated Decision Support system provides the user

with a personalized forecast of future blood glucose concentration over the next 8 hours. The forecasts were shown to be reasonably accurate, with 91% of predictions within 50 mg/dL of the glucometer readings and 75% within 27 mg/dL.<sup>[114]</sup> Thus, these predictions yield actionable information that can be used to guide future behavior and achieve better glycemic control.

Another example of this system architecture is the iTBra in development by Cyrcadia,<sup>[115]</sup> a smart bra developed for early detection of breast cancer. The iTBra contains two breast-conforming patches with integrated thermistor sensors that track local metabolic activity and the fluctuations in skin temperature associated with the circadian rhythm, measures that are known to relate to breast cancer progression.<sup>[116]</sup> After wearing the device for two hours, the skin temperature rhythm data is transmitted to the smartphone then uploaded to the cloud for analysis where AI algorithms generate a diagnosis. Cyrcadia claims the diagnoses generated by the iTBra have an accuracy of 84% with a sensitivity and specificity of 90% and 84%, respectively.<sup>[60]</sup> While the results are unpublished, other works have demonstrated the feasibility of the approach.<sup>[117]</sup>

The Air Next by NuvoAir<sup>[118]</sup> is a smart spirometer used to monitor pulmonary function. The device provides clinically accurate measurements of forced expiratory volume in the first second (FEV1) and forced vital capacity (FVC) in addition to accurate detection of obstructive ventilatory impairment, with a sensitivity and specificity of 90% and 97%, respectively.<sup>[119]</sup> In a follow-up study looking at its use in low resource settings, the smart spirometer detected ventilatory impairment with a sensitivity and specificity of 98% and 74%, respectively.<sup>[120]</sup> While this core functionality uses only local processing, NuvoAir uses the cloud to generate personalized care suggestions using their Lung Health AI platform. The DUO by Eko<sup>[121]</sup> is an upcoming example of this system architecture. The DUO is an FDA cleared and HIPAA compliant device that combines a digital stethoscope with a 1-lead ECG. While the core data processing is performed locally on-device with results sent to the smartphone via Bluetooth., Eko has announced that soon cloud-based machine learning will be used to perform automated data analysis.

CloudMinds has developed a smartphone-integrated cloud-based Raman spectrometer called the XI.<sup>[122, 123]</sup> The spectrometer is fully integrated with the back of a custom Android smartphone and is connected to the phone via WiFi, Bluetooth, or 4G data connection. The acquired Raman spectra along with the background signal is transmitted to a cloud server for background subtraction and material identification using a proprietary deep learning model. The authors also state that their system can function as a standalone unit without relying on the cloud server for analysis at the cost of increased compute time. This makes their system possess characteristics of both a tethered and hub architecture. They have shown that their platform was able to identify a single unknown material with an accuracy of 99.9%, mixture of two materials with an accuracy of 96.7%, and a mixture of three materials with an accuracy of 85.7%.<sup>[123]</sup>

### 3. Future Directions and Challenges

As the digital health paradigm gains traction, mHealth devices used by patients and consumers will contain increasingly advanced biosensors for measuring a large range of personal health parameters, expanding upon the current set of vital signs and biochemical measurements. Amidst this anticipated proliferation of smartphone-based mHealth devices, we describe for researchers in biosensors four system architectures that could help constrain the specifications of the biosensor. This perspective aligns with that of data informatics researchers in mHealth,<sup>[27]</sup> and concurs with the “sample-to-answer” workflow (i.e. from the acquisition of signal from a clinical sample to processing the data to yield health information of interest) which is sought after in an integrated POC diagnostics device.<sup>[124]</sup> Specifically, by examining the flow of data through the sample-to-answer workflow, this categorization contextualizes how the biosensor fits into the broad architecture of the mHealth device. (While this review provides examples of applications that fall under each of these four categories, the review is not meant to be an exhaustive survey of biosensors used in personal mobile health space.)

How would a researcher assess which system architecture would be the most appropriate, given a target health parameter to sense? Depending on the use case (for example, whether a highly sensitive and precise value is required for clinical diagnosis, versus binning of results or observation of a general trend for maintaining general wellness), the required technical specifications may be achievable as a built-in biosensor on the phone, even if an off-phone biosensor could produce more analytically powerful measurements (see the “on-phone” and “off-phone” specifications in Table 1). In the “integrated” architecture, the biosensor fits into the phone and directly interfaces with its circuitry, with ideally an overall compact device for the end user. By contrast, in a “tethered” architecture where the biosensor is separate from the smartphone, the construction of the biosensor can take on a large number of materials and designs, but data connectivity must also be built into the biosensor.

Similarly, there are implications for biosensor development when considering data processing. As the processing power of smartphones increases over time, the data processing may become less reliant on server computing to favor mHealth devices of the “integrated” and “tethered” architectures. For example, mHealth devices could take advantage of deep-learning frameworks that enable AI models to be run directly on the phone<sup>[125]</sup> to decrease the time to answer, enable offline use, and reduce server cost. Biosensors that provide data in forms that are readily processed locally would harmonize with these two architectures. On the other hand, the advent of 5G networks, which can reach 10 Gbit/s data transfer rates (more than a 20-fold increase over LTE) with a latency of around 3 ms (compared to 50 ms for LTE), will enable the transfer of greater amounts of data to the cloud for processing.<sup>[126]</sup> The increase in data transfer speeds and reduction in network latency will support the burgeoning field of minimally invasive, non-obtrusive continuous biosensors. The capability to collect large quantities of meaningful health parameters in real time and transfer them to a server for advanced data analytics will further support the vision of mHealth to shift from diagnosing illness to predicting adverse events in advance. The development of continuous biosensors in this data network environment could help shift the paradigm of healthcare from reactive to proactive patient care.

Finally, roadblocks must be addressed before personal mHealth sensors can achieve widespread use. First, usability studies will need to be carried out that analyze user feedback on different aspects of the device and software to identify and correct points of failure.<sup>[127]</sup> In many cases, current devices have only been tested in controlled environments and have not been validated with the target audience. Usability studies will also help capture issues stemming from variations in the manufacture specifications of smartphone hardware. Next, careful regulation must protect users from unsafe applications (an example being a blood pressure measurement application that was withdrawn due to dangerously inaccurate predictions).<sup>[128]</sup> Additionally, with the rise of AI, it is important to ensure that the predictive models are accurate. Since the accuracy of data-driven models are dependent on the dataset that was used for training, biased datasets could skew the model and lead to identifying trends and patterns that are not applicable to the user.<sup>[129]</sup> So far, for “software as a medical device”, the FDA has approved only locked algorithms (which provide identical results each time given the same input, with examples being static look-up tables and decision trees).<sup>[130]</sup>

According to the 2015 guideline issued by the FDA<sup>[29, 131]</sup>, all applications that, by using their internal or external sensors, can turn a smartphone into a medical device will need to be regulated by the FDA. Since a number of the examples detailed in this review fall under the medical device category, it is necessary that the researchers keep in mind the regulatory processes and its requirements for the commercialization of the device. The health data generated by the systems would be classified as protected health information and, as such, would require the cloud databases used to store the sensitive data to have the necessary encryptions in place to ensure that they are compliant to the Health Insurance Portability and Accountability Act. Majumder and Deen have, in their review, presented a detailed summary of the state of the regulatory policies for mHealth devices in the US and UK.<sup>[29]</sup> Kotz *et al.* have presented a detailed look into the privacy and security challenges presented by mHealth technology.<sup>[132]</sup> For AI and machine learning, the FDA is considering to emphasize a well-established algorithm change protocol and validation process, such that algorithms can learn and change while remaining safe and effective.<sup>[130]</sup> Moreover, patient privacy and data security must be ensured.<sup>[132, 133]</sup> With increasing use of AI, the models may leak identifiable user information from the training data due to unintended memorization.<sup>[134]</sup> As biosensors are increasingly developed with connected hardware and software towards use in decentralized settings, it will become important for researchers to be aware of the features of the chosen system architecture, including data security, while collecting and analyzing personal health information.

## Acknowledgements

S.A. and D.C. contributed equally to this work. This work was supported in part by the National Institute of Health (grant number: 1R01HD088156, 2R44AI096551) and the National Science Foundation Graduate Research Fellowship under Grant No. DGE – 1644869.

## Biography

**Samuel Sia**, a Professor of Biomedical Engineering at Columbia University, develops technologies for point-of-care blood tests, wearable sensors, implantable devices, and cell-



based therapy. He is the founder of Claros Diagnostics (which was acquired by OPKO Health, and which developed a now FDA-approved prostate cancer diagnostics device) and Harlem Biospace, a life-science incubator in New York City. Dr Sia has a B.Sc. in Biochemistry from the University of Alberta, and a PhD in Biophysics as an HHMI predoctoral fellow from Harvard University. Dr Sia completed a postdoctoral fellowship in Chemistry and Chemical Biology at Harvard University.



## References

- [1]. Wood CS, Thomas MR, Budd J, Mashamba-Thompson TP, Herbst K, Pillay D, Peeling RW, Johnson AM, McKendry RA, Stevens MM, Nature 2019, 566, 467. [PubMed: 30814711]
- [2]. Sackmann EK, Fulton AL, Beebe DJ, Nature 2014, 507, 181. [PubMed: 24622198]
- [3]. Nayak S, Blumenfeld NR, Laksanasopin T, Sia SK, Anal Chem 2017, 89, 102. [PubMed: 27958710]
- [4]. Thuau D, Ducrot PH, Poulin P, Dufour I, Ayela C, Micromachines (Basel) 2018, 9;Bogue R, Sensor Rev 2013, 33, 300;Ciuti G, Ricotti L, Menciassi A, Dario P, Sensors-Basel 2015, 15, 6441. [PubMed: 25808763]
- [5]. Nge PN, Rogers CI, Woolley AT, Chem Rev 2013, 113, 2550. [PubMed: 23410114]
- [6]. Zhong Q, Ding H, Gao B, He Z, Gu Z, Advanced Materials Technologies 2019, 4, 1800663;Chaves R, Sia SK, Clin Chem 2018, 64, 1125. [PubMed: 29222340]
- [7]. Holzinger M, Le Goff A, Cosnier S, Front Chem 2014, 2;Lu SM, Yu T, Wang YM, Liang LG, Chen Y, Xu F, Wang SQ, Analyst 2017, 142, 3309; [PubMed: 28828428] Kim YS, Raston NHA, Gu MB, Biosens Bioelectron 2016, 76, 2; [PubMed: 26139320] Lan LY, Yao Y, Ping JF, Ying YB, Biosens Bioelectron 2017, 91, 504; [PubMed: 28082239] Pan MF, Gu Y, Yun YG, Li M, Jin XC, Wang S, Sensors-Basel 2017, 17;Suvarnaphaet P, Pechprasarn S, Sensors-Basel 2017, 17.
- [8]. Wang BZ, Akiba U, Anzai J, Molecules 2017, 22.
- [9]. Batool R, Rhouati A, Nawaz MH, Hayat A, Marty JL, Biosensors (Basel) 2019, 9;Taguchi M, Ptitsyn A, McLamore ES, Claussen JC, J Diabetes Sci Technol 2014, 8, 403. [PubMed: 24876594]
- [10]. Holst A, Number of smartphones sold to end users worldwide from 2007 to 2020, <https://www.statista.com/statistics/263437/global-smartphone-sales-to-end-users-since-2007/>, accessed: August, 2019.
- [11]. [bankmycell.com](https://www.bankmycell.com/blog/how-many-phones-are-in-the-world/), HOW MANY PHONES ARE IN THE WORLD?, [https://www.bankmycell.com/blog/how-many-phones-are-in-the-world](https://www.bankmycell.com/blog/how-many-phones-are-in-the-world/), accessed: August, 2019.
- [12]. Center PR, Mobile Fact Sheet, <https://www.pewinternet.org/fact-sheet/mobile/>, accessed: August, 2019.
- [13]. Hernandez-Neuta I, Neumann F, Brightmeyer J, Tis TB, Madaboosi N, Wei Q, Ozcan A, Nilsson M, J Intern Med 2019, 285, 19. [PubMed: 30079527]
- [14]. Dimitrov DV, Healthc Inform Res 2016, 22, 156; [PubMed: 27525156] Darwish A, Hassanien AE, Elhoseny M, Sangaiah AK, Muhammad K, J Amb Intel Hum Comp 2019, 10, 4151;Haughey J, Taylor K, Dohrmann M, Snyder G, Deloitte, 2018.
- [15]. Song JZ, Pandian V, Mauk MG, Bau HH, Cherry S, Tisi LC, Liu CC, Anal Chem 2018, 90, 4823. [PubMed: 29542319]
- [16]. Frumusanu A, Arm Unveils Client CPU Performance Roadmap Through 2020, <https://www.anandtech.com/show/13226/arm-unveils-client-cpu-performance-roadmap>, accessed:

- August, 2019;Triggs R, Need for speed: how much faster are modern phone processors, <https://www.androidauthority.com/smartphone-benchmarks-by-age-995777/>, accessed: August, 2019.
- [17]. Griebel L, Prokosch HU, Kopcke F, Toddenroth D, Christoph J, Leb I, Engel I, Sedlmayr M, Bmc Med Inform Decis 2015, 15;Hashem IAT, Yaqoob I, Anuar NB, Mokhtar S, Gani A, Khan SU, Inform Syst 2015, 47, 98.
- [18]. N. S. Foundation, Smart and Connected Health (SCH) Connecting Data, People and Systems, <https://www.nsf.gov/pubs/2018/nsf18541/nsf18541.htm>, accessed: August, 2019.
- [19]. Sun AC, Hall DA, Electroanal 2019, 31, 2.
- [20]. Ozcan A, Lab Chip 2014, 14, 3187. [PubMed: 24647550]
- [21]. Quesada-Gonzalez D, Merkoci A, Biosens Bioelectron 2017, 92, 549; [PubMed: 27836593] Xu XY, Akay A, Wei HL, Wang SQ, Pinguan-Murphy B, Erlandsson BE, Li XJ, Lee W, Hu J, Wang L, Xu F, P Ieee 2015, 103, 236.
- [22]. Kobori Y, Pfanner P, Prins GS, Niederberger C, Fertil Steril 2016, 106, 574; [PubMed: 27336208] Hergemoller T, Laumann D, Phys Teach 2017, 55, 361.
- [23]. Rivenson Y, Koydemir HC, Wang HD, Wei ZS, Ren ZS, Gunaydin H, Zhang YB, Gorocs Z, Liang K, Tseng D, Ozcan A, Acs Photonics 2018, 5, 2354.
- [24]. Xu DD, Huang XW, Guo JH, Ma X, Biosens Bioelectron 2018, 110, 78. [PubMed: 29602034]
- [25]. Kwon L, Long KD, Wan Y, Yu H, Cunningham BT, Biotechnol Adv 2016, 34, 291. [PubMed: 26952640]
- [26]. Wire B, Healthcare Primed to Become the Fastest Growing Sector, <https://www.businesswire.com/news/home/20181126005585/en/Seagate-Launches-New-Data-Readiness-Index-Revealing-Impact>, accessed: August, 2019.
- [27]. Jovanov E, Zhang Y, IEEE Transactions on Information Technology in Biomedicine 2004, 8, 405. [PubMed: 15615031]
- [28]. Shin J, Chakravarty S, Choi W, Lee K, Han D, Hwang H, Choi J, Jung HI, Analyst 2018, 143, 1515; [PubMed: 29536992] Gambhir SS, Ge TJ, Vermesh O, Spitler R, Sci Transl Med 2018, 10;Seo SE, Tabei F, Park SJ, Askarian B, Kim KH, Moallem G, Chong JW, Kwon OS, J Ind Eng Chem 2019, 77, 1;Zarei M, Trac-Trend Anal Chem 2017, 91, 26;Ozcan A, McLeod E, Annu Rev Biomed Eng 2016, 18, 77. [PubMed: 27420569]
- [29]. Majumder S, Deen MJ, Sensors-Basel 2019, 19.
- [30]. Gu CZ, Sensors-Basel 2016, 16.
- [31]. Guissi S, CMOS Image Sensors (CIS): Past, Present & Future, <https://www.coventor.com/blog/cmos-image-sensors-cis-past-present-future/>, accessed: August, 2019;Skorka O, Joseph D, Sensors (Basel) 2011, 11, 4512. [PubMed: 22163860]
- [32]. Qu H, Micromachines (Basel) 2016, 7.
- [33]. AZoNano, Applications of Silicon in MEMS Devices, Applications of Silicon in MEMS Devices, accessed: August, 2019.
- [34]. Ren KN, Zhou JH, Wu HK, Accounts Chem Res 2013, 46, 2396;Roy E, Pallandre A, Zribi B, Horny MC, Delapierre FD, Cattoni A, Gamby J, Haghiri-Gosnet AM, Advances in Microfluidics - New Applications in Biology, Energy, and Materials Sciences 2016, 335.
- [35]. Liu X, Lin B, in Encyclopedia of Microfluidics and Nanofluidics, (Ed: Li D), Springer New York, New York, NY 2015, 1723.
- [36]. Qualcomm, Snapdragon System-in-Package, <https://www.qualcomm.com/products/snapdragon-system-package>, accessed: August, 2019.
- [37]. Qualcomm, Snapdragon Platform Comparison, <https://www.qualcomm.com/snapdragon/processors/comparison>, accessed: August, 2019.
- [38]. Kalwa U, Legner C, Kong T, Pandey S, Symmetry-Basel 2019, 11.
- [39]. MetaOptima, MoleScope product page, <https://molescope.com/product/>, accessed: August, 2019.
- [40]. Abbott LM, Smith SD, Australas J Dermatol 2018, 59, 168. [PubMed: 29292506]
- [41]. Xu XY, Ding WX, Wang XM, Cao RF, Zhang MY, Lv PL, Xu F, Sci Rep-Uk 2016, 6.
- [42]. Lee SA, Yang CH, Lab Chip 2014, 14, 3056. [PubMed: 24964209]
- [43]. Orth A, Wilson ER, Thompson JG, Gibson BC, Sci Rep-Uk 2018, 8.

- [44]. D'Ambrosio MV, Bakalar M, Bennuru S, Reber C, Skandarajah A, Nilsson L, Switz N, Kamgno J, Pion S, Boussinesq M, Nutman TB, Fletcher DA, *Sci Transl Med* 2015, 7.
- [45]. Kanakasabapathy MK, Sadasivam M, Singh A, Preston C, Thirumalaraju P, Venkataraman M, Bormann CL, Draz MS, Petrozza JC, Shafiee H, *Sci Transl Med* 2017, 9.
- [46]. Halvorsen CP, Olson L, Araujo AC, Karlsson M, Nguyen TT, Khu DTK, Le HTT, Nguyen HTB, Winbladh B, Russom A, *Sci Rep-Uk* 2019, 9.
- [47]. Priye A, Bird SW, Light YK, Ball CS, Negrete OA, Meagher RJ, *Sci Rep-Uk* 2017, 7.
- [48]. Thap T, Chung H, Jeong C, Hwang KE, Kim HR, Yoon KH, Lee J, *Sensors-Basel* 2016, 16.
- [49]. Chandrasekhar A, Natarajan K, Yavarimanesh M, Mukkamala R, *Sci Rep-Uk* 2018, 8.
- [50]. Chandrasekhar A, Kim CS, Naji M, Natarajan K, Hahn JO, Mukkamala R, *Sci Transl Med* 2018, 10.
- [51]. Oculocare, Alleye smartphone application, <https://alleye.io/>, accessed: August, 2019; V. A. a. Science, myVisionTrack, <https://myvisiontrack.com/>, accessed: August, 2019.
- [52]. Rutter LM, Nouzova E, Stott DJ, Weir CJ, Assi V, Barnett JH, Clarke C, Duncan N, Evans J, Green S, Hendry K, McGinlay M, McKeever J, Middleton DG, Parks S, Shaw R, Tang E, Walsh T, Weir AJ, Wilson E, Quasim T, MacLulich AMJ, Tiegies Z, *Bmc Geriatr* 2018, 18.
- [53]. Lin YC, Lai YH, Chang HW, Tsao Y, Chang YP, Chang RY, *Ieee Syst J* 2018, 12, 20.
- [54]. Yetisen AK, Moreddu R, Seifi S, Jiang N, Vega K, Dong XC, Dong J, Butt H, Jakobi M, Elsner M, Koch AW, *Angew Chem Int Edit* 2019, 58, 10506.
- [55]. Berg B, Cortazar B, Tseng D, Ozkan H, Feng S, Wei QS, Chan RYL, Burbano J, Farooqui Q, Lewinski M, Di Carlo D, Garner OB, Ozcan A, *Acs Nano* 2015, 9, 7857. [PubMed: 26159546]
- [56]. Ding H, Chen C, Zhao HC, Yue Y, Han CY, *Analyst* 2019, 144, 4380. [PubMed: 31206108]
- [57]. Uthoff RD, Song BF, Sunny S, Patrick S, Suresh A, Kolor T, Keerthi G, Spires O, Anbarani A, Wilder-Smith P, Kuriakose MA, Birur P, Liang RG, *Plos One* 2018, 13.
- [58]. Iván JLR Balán C, Nayak Samiksha, Lentz Cody, Arumugam Siddarth, Kutner Bryan, Dolezal Curtis, Macar Ongun Uzay, Pabari Tejit, Ying Alexander Wang, Okrah Michael, Sia Samuel K. 2019.
- [59]. Wang X, Li F, Cai ZQ, Liu KF, Li J, Zhang BY, He JB, *Anal Bioanal Chem* 2018, 410, 2647. [PubMed: 29455281]
- [60]. Healthy.io, Home based urinalysis test kit, <https://healthy.io/>, accessed: August, 2019.
- [61]. Luo H, Yang DY, Barszczyk A, Vempala N, Wei J, Wu SJ, Zheng PP, Fu GY, Lee K, Feng ZP, *Circ-Cardiovasc Imag* 2019, 12.
- [62]. Qompium, FibriCheck, <https://www.fibrichk.com/>, accessed: August, 2019; Proesmans T, Mortelmans C, Van Haelst R, Verbrugge F, Vandervoort P, Vaes B, *Jmir Mhealth Uhealth* 2019, 7.
- [63]. Sharma J, Ono T, Yukino R, Miyashita H, Hanyu N, Handa H, Sandhu A, *Biomed Phys Eng Expr* 2019, 5.
- [64]. Narayan S, Shidare P, Niranjana T, Williams K, Freudman J, Sehra R, *Sleep Breath* 2019, 23, 269. [PubMed: 30022325]
- [65]. S. IO, Steth IO, <https://stethio.com/>, accessed: August, 2019.
- [66]. R. Health, ResApp, <https://www.resapphealth.com.au/>, accessed: August, 2019.
- [67]. hearX, hearScreen, <https://www.hearxgroup.com/hearscreen/>, accessed: August, 2019.
- [68]. Louw C, Swanepoel DW, Eikelboom RH, Myburgh HC, *Ear Hearing* 2017, 38, E93. [PubMed: 27764002]
- [69]. Faurholt-Jepsen M, Busk J, Porarinsdottir H, Frost M, Bardram JE, Vinberg M, Kessing LV, *Aust Nz J Psychiat* 2019, 53, 119.
- [70]. Zhang DM, Lu YL, Zhang Q, Liu L, Li S, Yao Y, Jiang J, Liu GL, Liu QJ, *Sensor Actuat B-Chem* 2016, 222, 994; Bandodkar AJ, Molinnus D, Mirza O, Guinovart T, Windmiller JR, Valdes-Ramirez G, Andrade FJ, Schoning MJ, Wang J, *Biosens Bioelectron* 2014, 54, 603; [PubMed: 24333582] Wang XH, Lin GH, Cui GZ, Zhou XF, Liu GL, *Biosens Bioelectron* 2017, 90, 549; [PubMed: 27825884] Sun A, Wambach T, Venkatesh AG, Hall DA, *IEEE Biomed Circuits Syst Conf* 2014, 2014, 312; [PubMed: 26097899] Lillehoj PB, Huang MC, Truong N, Ho CM, *Lab*

- Chip 2013, 13, 2950; [PubMed: 23689554] Zhang L, Yang W, Yang Y, Liu H, Gu Z, Analyst 2015, 140, 7399. [PubMed: 26415134]
- [71]. Huang X, Xu D, Chen J, Liu J, Li Y, Song J, Ma X, Guo J, Analyst 2018, 143, 5339. [PubMed: 30327808]
- [72]. Deng WP, Dou YZ, Song P, Xu H, Aldalbahi A, Chen N, El-Sayed NN, Gao JM, Lu JX, Song SP, Zuo XL, J Electroanal Chem 2016, 777, 117.
- [73]. Guo J, Anal Chem 2017, 89, 8609. [PubMed: 28825471]
- [74]. Liu L, Zhang DM, Zhang Q, Chen X, Xu G, Lu YL, Liu QJ, Biosens Bioelectron 2017, 93, 94. [PubMed: 27712992]
- [75]. Talukder N, Furniturewalla A, Le T, Chan M, Hirday S, Cao X, Xie P, Lin Z, Gholizadeh A, Orbine S, Javanmard M, Biomed Microdevices 2017, 19, 36. [PubMed: 28432532]
- [76]. Escobedo P, Erenas MM, Martinez-Olmos A, Carvajal MA, Gonzalez-Chocano S, Capitan-Vallvey LF, Palma AJ, Biosens Bioelectron 2019, 141, 111360. [PubMed: 31176114]
- [77]. Hu L, Xu G, Chem Soc Rev 2010, 39, 3275. [PubMed: 20593100]
- [78]. Kassal P, Kim J, Kumar R, de Araujo WR, Steinberg IM, Steinberg MD, Wang J, Electrochem Commun 2015, 56, 6.
- [79]. Kassal P, Zubak M, Scheipl G, Mohr GJ, Steinberg MD, Steinberg IM, Sensor Actuat B-Chem 2017, 246, 455.
- [80]. Laksanasopin T, Guo TW, Nayak S, Sridhara AA, Xie S, Olowookere OO, Cadinu P, Meng FX, Chee NH, Kim J, Chin CD, Munyazesa E, Mugwaneza P, Rai AJ, Mugisha V, Castro AR, Steinmiller D, Linder V, Justman JE, Nsanzimana S, Sia SK, Sci Transl Med 2015, 7.
- [81]. Li J, Sun YJ, Chen C, Sheng T, Liu P, Zhang GB, Anal Chim Acta 2019, 1052, 105. [PubMed: 30685028]
- [82]. Das A, Swedish T, Wahi A, Moufarrej M, Noland M, Gurry T, Aranda-Michel E, Aksel D, Wagh S, Sadashivaiah V, Zhang X, Raskar R, Proc Spie 2015, 9482.
- [83]. Reyes BA, Olvera-Montes N, Charleston-Villalobos S, Gonzalez-Camarena R, Mejia-Avila M, Aljama-Corrales T, Sensors-Basel 2018, 18.
- [84]. Jayatilake D, Ueno T, Teramoto Y, Nakai K, Hidaka K, Ayuzawa S, Eguchi K, Matsumura A, Suzuki K, Ieee J Transl Eng He 2015, 3.
- [85]. Huang CC, Lee PY, Chen PY, Liu TY, Ieee T Ultrason Ferr 2012, 59, 182.
- [86]. Stopczynski A, Stahlhut C, Larsen JE, Petersen MK, Hansen LK, Plos One 2014, 9.
- [87]. McKenzie ED, Lim ASP, Leung ECW, Cole AJ, Lam AD, Eloyan A, Nirola DK, Tshering L, Thibert R, Garcia RZ, Bui E, Deki S, Lee L, Clark SJ, Cohen JM, Mantia J, Brizzi KT, Sorets TR, Wahlster S, Borzello M, Stopczynski A, Cash SS, Mateen FJ, Sci Rep-Uk 2017, 7.
- [88]. Fitbit, Aria 2, <https://www.fitbit.com/aria2>, accessed: August, 2019.
- [89]. Apple, Apple Watch, <https://www.apple.com/watch/>, accessed: August, 2019.
- [90]. Samsung, Galaxy Watch, <https://www.samsung.com/global/galaxy/galaxy-watch/>, accessed: August, 2019.
- [91]. Thomson EA, Nuss K, Comstock A, Reinwald S, Blake S, Pimentel RE, Tracy BL, Li KG, J Sport Sci 2019, 37, 1411; Benedetto S, Caldato C, Bazzan E, Greenwood DC, Pensabene V, Actis P, Plos One 2018, 13; Feehan LM, Geldman J, Sayre EC, Park C, Ezzat AM, Yoo Y, Hamilton CB, Li LC, Jmir Mhealth Uhealth 2018, 6.
- [92]. AliveCor, KardiaMobile, <https://www.alivecor.com/kardiamobile/>, accessed: August, 2019.
- [93]. William AD, Kanbour M, Callahan T, Bhargava M, Varma N, Rickard J, Saliba W, Wolski K, Hussein A, Lindsay BD, Wazni OM, Tarakji KG, Heart Rhythm 2018, 15, 1561. [PubMed: 30143448]
- [94]. Bumgarner J, Lambert C, Cantillon D, Baranowski B, Wolski K, Hussein A, Wazni O, Lindsay B, Tarakji K, J Am Coll Cardiol 2018, 71, 411.
- [95]. Qardio, QardioCore, <https://www.getqardio.com/qardiocore-wearable-ecg-ekg-monitor-iphone/>, accessed: August, 2019.
- [96]. BBBtech, elemark, <https://www.bbbtech.com/elemark>, accessed: August, 2019.
- [97]. Yun K, Choi J, Song IU, Chung YA, Appl Sci-Basel 2019, 9.

- [98]. Withings, Body+, <https://www.withings.com/us/en/body-plus>, accessed: August, 2019.
- [99]. Duren DL, Sherwood RJ, Czerwinski SA, Lee M, Choh AC, Siervogel RM, Cameron Chumlea W, J Diabetes Sci Technol 2008, 2, 1139. [PubMed: 19885303]
- [100]. Campo D, Khettab H, Yu R, Genain N, Edouard P, Buard N, Boutouyrie P, Am J Hypertens 2017, 30, 876. [PubMed: 28520843]
- [101]. Qardio, QardioArm, <https://www.getqardio.com/qardioarm-blood-pressure-monitor-iphone-android/>, accessed: August, 2019.
- [102]. Omron, HeartGuide, <https://omronhealthcare.com/products/heartguide-wearable-blood-pressure-monitor-bp8000m/>, accessed: August, 2019.
- [103]. Muse, Muse 2, <https://choosemuse.com/muse-2/>, accessed: August, 2019.
- [104]. H. C. Originals, ADAMM, <http://healthcareoriginals.com/solutions/#top>, accessed: August, 2019.
- [105]. i. Labs, iHealth Smart, <https://ihealthlabs.com/glucometer/wireless-smart-gluco-monitoring-system/>, accessed: August, 2019.
- [106]. DardioHealth, Smart Meter, <https://mydario.com/smart-meter/>, accessed: August, 2019.
- [107]. C. Medical, InPen, <https://www.companionmedical.com/inpen>, accessed: August, 2019.
- [108]. Klonoff DC, Kerr D, J Diabetes Sci Technol 2018, 12, 551. [PubMed: 29411641]
- [109]. Philips, Lumify, <https://www.usa.philips.com/healthcare/sites/lumify>, accessed: August, 2019.
- [110]. B. Network, iQ, <https://www.butterflynetwork.com/iq>, accessed: August, 2019.
- [111]. Poplin R, Varadarajan AV, Blumer K, Liu Y, McConnell MV, Corrado GS, Peng L, Webster DR, Nat Biomed Eng 2018, 2, 158; [PubMed: 31015713] Rajkomar A, Oren E, Chen K, Dai AM, Hajaj N, Hardt M, Liu PJ, Liu X, Marcus J, Sun M, Sundberg P, Yee H, Zhang K, Zhang Y, Flores G, Duggan GE, Irvine J, Le Q, Litsch K, Mossin A, Tansuwan J, Wexler Wang, J., Wilson J, Ludwig D, Volchenboum SL, Chou K, Pearson M, Madabushi S, Shah NH, Butte AJ, Howell MD, Cui C, Corrado GS, Dean J, NPJ Digit Med 2018, 1, 18. [PubMed: 31304302]
- [112]. Phillips C, Liaqat D, Gabel M, de Lara E, arXiv preprint arXiv:1906.07545 2019.
- [113]. O. Drop, Glucose Meter, <https://onedrop.today/products/glucose-meter>, accessed: August, 2019.
- [114]. Goldner DR, Osborn CY, Sears LE, Huddleston B, Dachis J, Diabetes 2018, 67.
- [115]. C. Asia, iTBra, <https://cycradia.asia/itbra/>, accessed: August, 2019.
- [116]. Li S, Ao X, Wu H, Chin J Cancer Res 2013, 25, 442; [PubMed: 23997531] Salhab M, Al Sarakbi W, Mokbel K, Int Semin Surg Oncol 2005, 2, 8. [PubMed: 15819982]
- [117]. Salhab M, Keith LG, Laguens M, Reeves W, Mokbel K, Int Semin Surg Oncol 2006, 3, 8; [PubMed: 16584542] Ng EYK, Acharya UR, Kelth LG, Lockwood S, Inform Sciences 2007, 177, 4526.
- [118]. NuvoAir, Air Next, <https://shop.nuvoair.com/products/air-next-spirometer>, accessed: August, 2019.
- [119]. Ramos Hernandez C, Nunez Fernandez M, Pallares Sanmartin A, Mouronte Roibas C, Cerdeira Dominguez L, Botana Rial MI, Blanco Cid N, Fernandez Villar A, Plos One 2018, 13, e0192789. [PubMed: 29474502]
- [120]. du Plessis E, Swart F, Maree D, Heydenreich J, van Heerden J, Esterhuizen TM, Irusen EM, Koegelenberg CFN, Samj S Afr Med J 2019, 109, 219. [PubMed: 31084684]
- [121]. Eko, DUO, <https://ekohealth.com/duo/>, accessed: August, 2019.
- [122]. CloudMinds, XI, World's First Cloud AI Raman Spectrometer, <https://www.airaman.com/>, accessed: August, 2019; Mu TT, Li S, Feng HH, Zhang CC, Wang B, Ma X, Guo JH, Huang B, Zhu LQ, Ieee J Sel Top Quant 2019, 25.
- [123]. Chandler L, Huang B, Mu TT, "A smart handheld Raman spectrometer with cloud and AI deep learning algorithm for mixture analysis", presented at Next-Generation Spectroscopic Technologies XII, 2019.
- [124]. Chin CD, Linder V, Sia SK, Lab Chip 2012, 12, 2118; [PubMed: 22344520] Derda R, Gitaka J, Klapperich CM, Mace CR, Kumar AA, Lieberman M, Linnes JC, Jores J, Nasimolo J, Ndung'u J, Taracha E, Weaver A, Weibel DB, Kariuki TM, Yager P, Plos Neglect Trop D 2015, 9.



- [125]. Google, Bringing you the next-generation Google Assistant, <https://blog.google/products/assistant/next-generation-google-assistant-io/>, accessed: August, 2019.
- [126]. D. Telekom, 5G speed is data transmission in real time, <https://www.telekom.com/en/company/details/5g-speed-is-data-transmission-in-real-time-544498>, accessed: August, 2019.
- [127]. Nayak S, Guo T, Lopez-Rios J, Lentz C, Arumugam S, Hughes J, Dolezal C, Linder V, Carballo-Dieguez A, Balan IC, Sia SK, Lab Chip 2019, 19, 2241. [PubMed: 31168548]
- [128]. Plante TB, O'Kelly AC, Urrea B, MacFarlane ZT, Blumenthal RS, Charleston J, Miller ER, Appel LJ, Martin SS, NPJ Digit Med 2018, 1, 31; [PubMed: 31304313] Plante TB, Urrea B, MacFarlane ZT, Blumenthal RS, Miller ER 3rd, Appel LJ, Martin SS, JAMA Intern Med 2016, 176, 700. [PubMed: 26938174]
- [129]. Courtland R, Nature 2018, 558, 357; [PubMed: 29925973] Wu X, Zhang X, arXiv preprint arXiv:1611.04135 2016, 4038.
- [130]. FDA, 2019.
- [131]. FDA, Policy for Device Software Functions and Mobile Medical Applications: Guidance for Industry and Food and Drug Administration Staff, <https://www.fda.gov/media/80958/download>, accessed: August, 2019; Shuren J, Patel B, Gottlieb S, JAMA 2018, 320, 337. [PubMed: 29971339]
- [132]. Kotz D, Gunter CA, Kumar S, Weiner JP, Computer 2016, 49, 22. [PubMed: 28344359]
- [133]. Coventry L, Branley D, Maturitas 2018, 113, 48; [PubMed: 29903648] Cummings E, Borycki EM, Roehrer E, Stud Health Technol 2013, 183, 227.
- [134]. Carlini N, Liu C, Kos J, Erlingsson Ú, Song D, arXiv preprint arXiv:1802.08232 2018.
- [135]. Samsung, Galaxy S10 Specifications, <https://www.samsung.com/global/galaxy/galaxy-s10/specs/>, accessed: August, 2019.
- [136]. Nikon, Z6, <https://www.nikonusa.com/en/nikon-products/product/mirrorless-cameras/z-6.html>, accessed: August, 2019.
- [137]. Dutta S, TrAC Trends in Analytical Chemistry 2018.
- [138]. ams, TSL2541 Ambient Light Sensor, <https://ams.com/tsl2541>, accessed: August, 2019.
- [139]. ams, TSL25911 Ambient Light Sensor, <https://ams.com/tsl25911>, accessed: August, 2019.
- [140]. Knowles, SPH0645LM4H-B, <https://www.knowles.com/docs/default-source/model-downloads/sph0645lm4h-b-datasheet-rev-c.pdf?Status=Master&sfvrsn=4>, accessed: August, 2019.
- [141]. M. Electronics, ICS-40300, <https://www.mouser.com/ProductDetail/TDK-InvenSense/ICS-40300?qs=sGAEpiMZZMsZoypmI867ETWGaEFM6%2F3p%252B%2FZaAXFnXIV4RLyiQg%3D%3D>, accessed: August, 2019.
- [142]. STMicroelectronics, LSM6DSL, <https://www.st.com/resource/en/datasheet/lsm6dsl.pdf>, accessed: August, 2019.
- [143]. A. Devices, ADXL356/ADXL357, <https://www.mouser.com/datasheet/2/609/ADXL356-357-1578586.pdf>, accessed: August, 2019.
- [144]. Fluke, Fluke 87V Industrial Multimeter, <https://www.fluke.com/en-us/product/electrical-testing/digital-multimeters/fluke-87v>, accessed: August, 2019.
- [145]. Gamry, Reference 3000, <https://www.gamry.com/potentiostats/reference-3000/>, accessed: August, 2019.
- [146]. Topas, Topas Cyclic Olefin Copolymer (COC), [https://topas.com/sites/default/files/files/TOPAS\\_Brochure\\_E\\_2014\\_06\(1\).pdf](https://topas.com/sites/default/files/files/TOPAS_Brochure_E_2014_06(1).pdf), accessed: August, 2019.



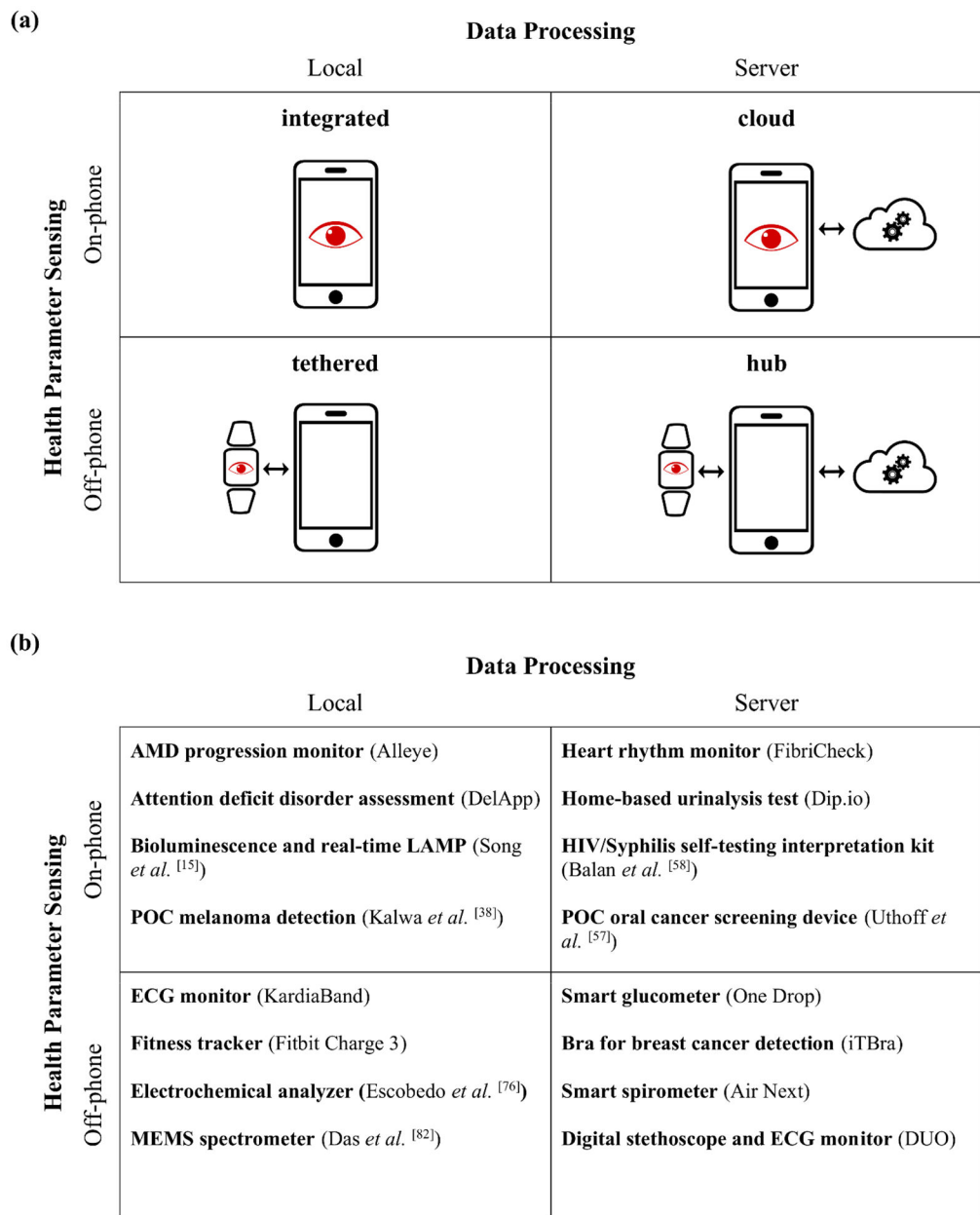


**Figure 1.** (a) Biosensors for collecting personal health data can be categorized into four distinct system architectures based on the method of sensing and processing health data. The categories are titled “integrated”, “cloud”, “tethered”, and “hub”. The red eye denotes general biosensing functionality (not just optical), which can be physically located on the phone or off the phone. Examples of on-phone sensors include smartphone-supplied cameras, ambient light sensors, microphones, accelerometers, gyroscopes, magnetometers, and barometers. (b) Examples of types of health sensing devices are shown for each system architecture.

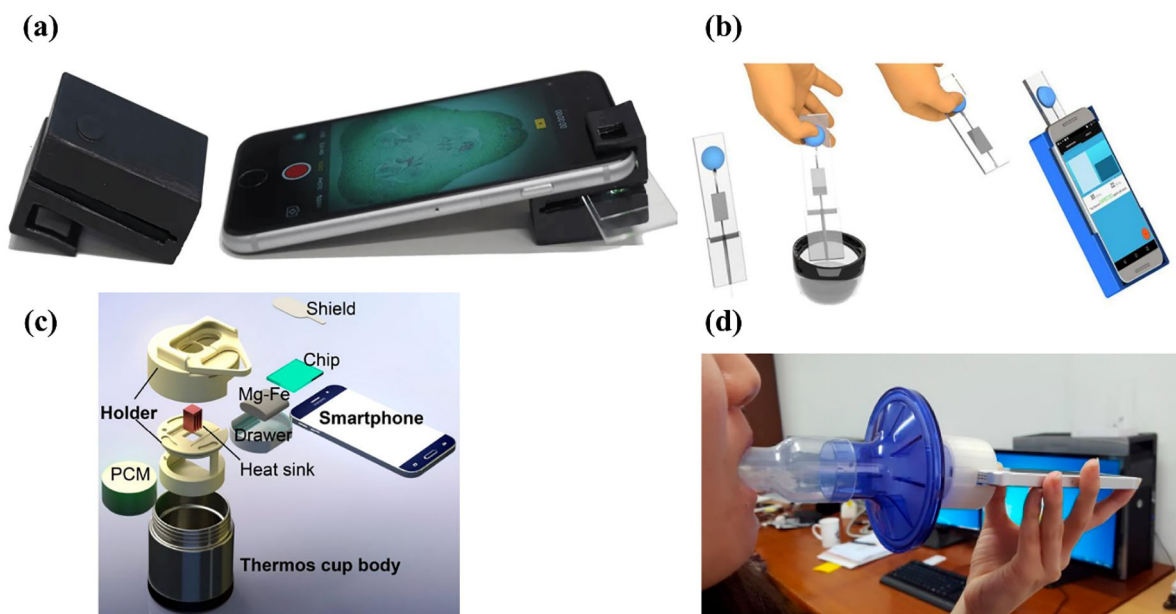


**Figure 2.** Examples of personal mobile health devices with biosensors built on the phone and data processed also locally on the phone. **(a)** Dual-mode microscope attachment (left) designed for the smartphone (right). Reproduced as is;<sup>[43]</sup> use permitted under the [Creative Commons Attribution License CC-BY 4.0](#) **(b)** Semen analyzer for point-of-care male fertility screening. Reproduced with permission;<sup>[45]</sup> Copyright 2017, The American Association for the Advancement of Science. **(c)** Smart-connected cup for rapid molecular diagnostics without the need for an excitation source or optical filters. Reprinted with permission;<sup>[15]</sup> Copyright 2018 American Chemical Society. **(d)** Smartphone device with mouthpiece attachment for lung function testing. Reproduced as is;<sup>[48]</sup> use permitted under the [Creative Commons Attribution License CC-BY 4.0](#)

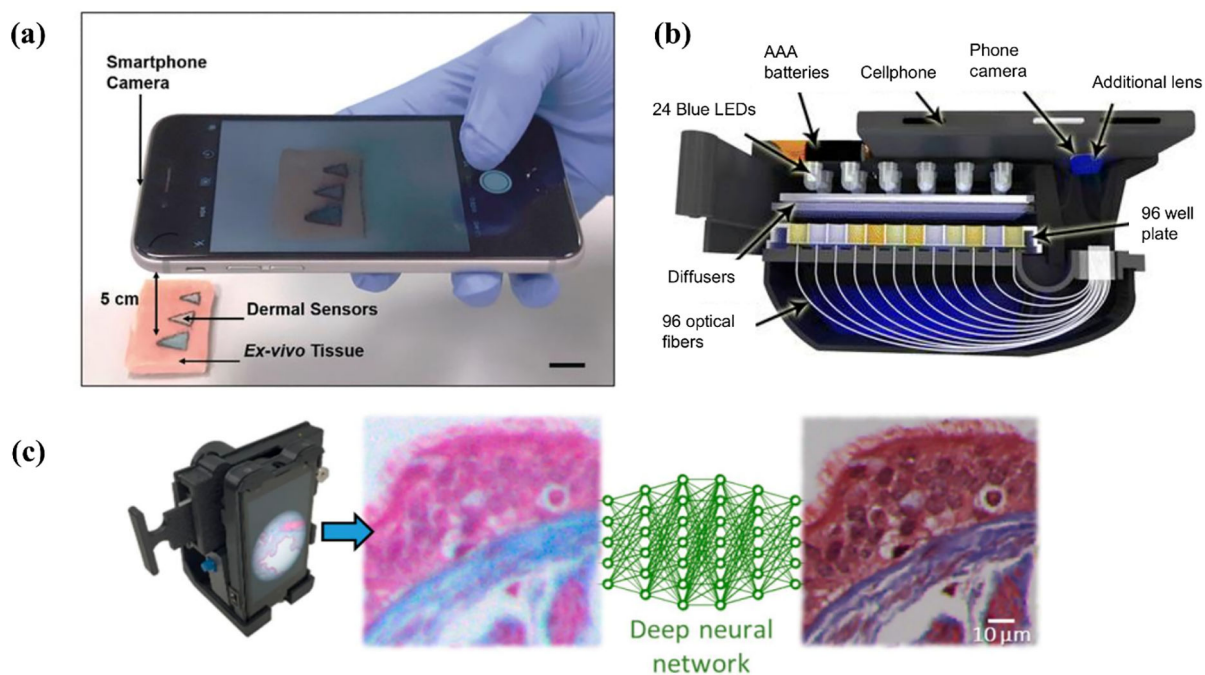


**Figure 3.**

Examples of personal mobile health devices with biosensing built on the phone but with data processed remotely on a server. **(a)** Injectable dermal tattoo sensors with a colorimetric readout for chemical analyte monitoring. Reproduced with permission.<sup>[54]</sup> Copyright 2019, John Wiley and Sons. **(b)** Smartphone-based microplate reader for point-of-care enzyme-linked immunosorbent assays. Reproduced with permission.<sup>[55]</sup> Copyright 2015, American Chemical Society (<https://pubs.acs.org/doi/10.1021/acsnano.5b03203>; further permissions related to the material excerpted should be directed to the ACS). **(c)** Smartphone microscope with the resolution of acquired images enhanced using a deep neural network. Reprinted with permission.<sup>[23]</sup> Copyright 2018, American Chemical Society.

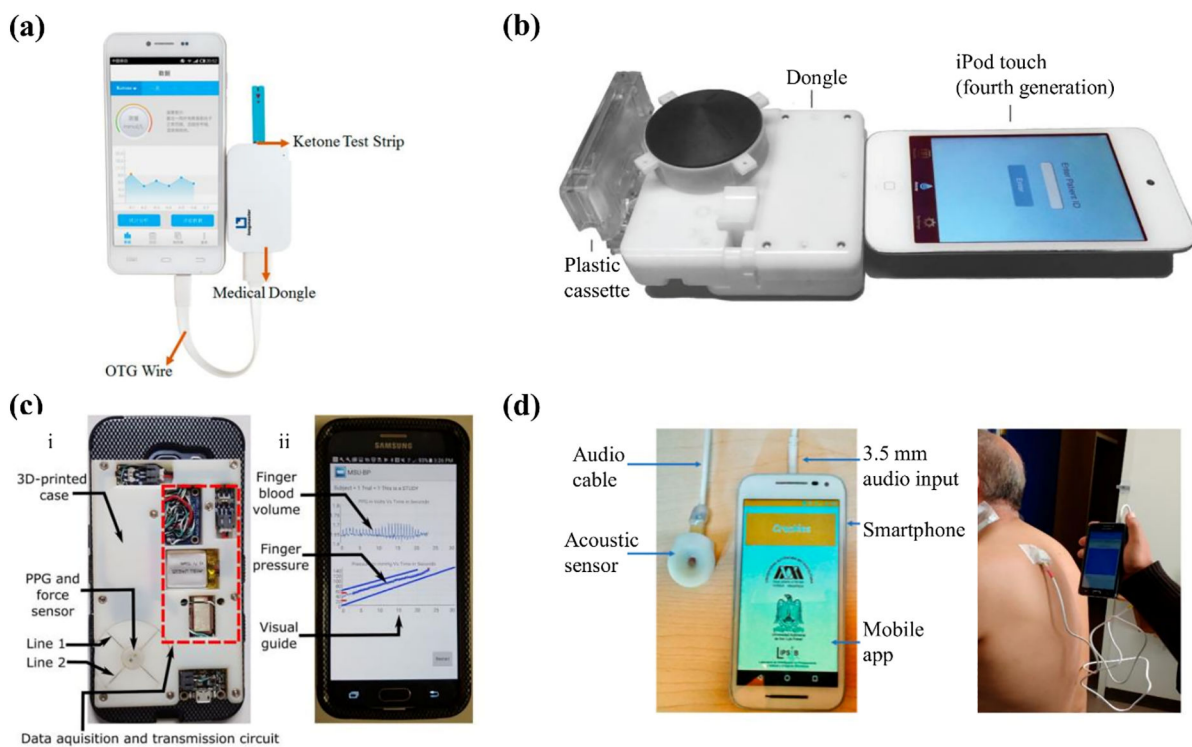


**Figure 4.** Examples of personal mobile health devices with biosensing built off the phone (for example, electrochemical sensing) as an accessory, and with data processed locally on the phone. **(a)** Amperometric-based system for blood ketone monitoring. Reproduced with permission.<sup>[73]</sup> Copyright 2017, American Chemical Society Group. **(b)** Portable diagnostics platform for point-of-care enzyme-linked immunosorbent assays. Reproduced with permission.<sup>[80]</sup> Copyright 2015, The American Association for the Advancement of Science. **(c)** Smartphone-based cuffless blood pressure monitor. (i) The smartphone attachment for off-phone sensing. (ii) The developed application for local processing. Reproduced with permission.<sup>[50]</sup> Copyright 2018, The American Association for the Advancement of Science. **(d)** System for automated detection of crackle sounds (left) demonstrated with a pneumonia patient (right). Reproduced as is;<sup>[83]</sup> use permitted under the [Creative Commons Attribution License CC-BY 4.0](https://creativecommons.org/licenses/by/4.0/)

**Table 1.** Table of biosensors for personal mobile health measurement devices summarizing function, key materials and properties, and technical specifications, both on- and off-phone.

Type of sensor	Example of measured health parameter	Technical Capability	SI Units	Class	Common Materials	Key Property	Typical Specifications	On-phone	Off-phone
<b>Camera</b>	Optical assay readout <sup>[38]</sup> or microscopy <sup>[42]</sup>	Record Image	-	CMOS	Silicon	Semiconductor/ photosensitive		16 <sup>[135]</sup>	24,5 <sup>[136]</sup>
					Silicon dioxide Polysilicon Phosphorus/Arsenic Boron/Gallium	Insulator Conductor N-type dopant P-type dopant	Resolution (MP)		
<b>Ambient Light Sensor</b>	Optical assay readout <sup>[137]</sup>	Measure ambient light	lx	CMOS	Silicon	Semiconductor/ photosensitive		60,000 <sup>[138]</sup>	88,000 <sup>[139]</sup>
					Silicon dioxide Polysilicon Phosphorus/Arsenic Boron/Gallium	Insulator Conductor N-type dopant P-type dopant	Range (lx)		
<b>Microphone</b>	Pulmonary function <sup>[48]</sup>	Record sound	-	MEMS	Silicon	Mature fabrication process	Range (kHz)	0.01–10 <sup>[140]</sup>	0.006–20 <sup>[141]</sup>
					Polysilicon	Ideal mechanical properties	Sensitivity (dB)	-26 <sup>[140]</sup>	-45 <sup>[141]</sup>
<b>Accelerometer</b>	Steps/activity <sup>[88]</sup>	Measures acceleration	m/s <sup>2</sup>	MEMS	Silicon	Mature fabrication process	Range (g)	±16 <sup>[142]</sup>	±40 <sup>[143]</sup>
					Polysilicon	Ideal mechanical properties	Sensitivity (mg/LSB)	0.488 <sup>[142]</sup>	0.078 <sup>[143]</sup>
<b>Voltmeter</b>	Electrocardiogram <sup>[92]</sup>	Measures electric potential	V	Digital	Silicon	Semiconductor/ photosensitive	Max voltage (V)	-	1000 <sup>[144]</sup>
					Silicon dioxide Polysilicon Phosphorus/Arsenic Boron/Gallium	Insulator Conductor N-type dopant P-type dopant	Max resolution DC/AC (µV)	-	10/100 <sup>[144]</sup>
<b>Potentiostat</b>	Electrochemical assays	Control electric potential and measure current	A	Digital	Gold, platinum, or glassy carbon	Inert for working electrode	Min current (pA)	-	300 <sup>[145]</sup>
					Silver/ silver chloride	Known potential for reference electrode	Max current (A)	-	3 <sup>[145]</sup>

Type of sensor	Example of measured health parameter	Technical Capability	SI Units	Class	Common Materials	Key Property	Typical Specifications	On-phone	Off-phone
					Platinum/graphite	Inert conductor for counter electrode	Max resolution (aA)	-	92 [145]
					Polydimethylsiloxane (PDMS)	Low-elastic modulus, gas permeable, good bonding properties, optical transparency, low cost, rapid fabrication	> 70% optical transmittance (nm)	-	400 – 700 [35]
					Cyclic olefin copolymer (COC)	Easy moldability, good optical transmission, low cost, biocompatibility, high chemical resistance, high heat resistance	> 70% optical transmittance (nm)	-	> 300 [146]
					Poly (methyl methacrylate) (PMMA)	Low price, rigid mechanical property, high optical transparency, easy fabrication	> 70% optical transmittance (nm)	-	400 – 700 [35]
<b>Microfluidics</b>	Recapitulate chemical assays at the point of care <sup>[80]</sup>	Run assay	-	-	Polycarbonate (PC)	High glass-transition temperature, optical transparency, low cost, high impact resistance, good machining properties	> 70% optical transmittance (nm)	-	400 – 700 [35]
					Glass	Biocompatible, optical transparency	> 70% optical transmittance (nm)	-	> 350 [35]
					Paper (Cellulose)	Cheap, abundant availability, biocompatible, white color provides good background for readouts	-	-	-